

Invited Speaker

1187 Probing the structure and dynamics of active molecular materials with cryo and liquid EM
Professor Joe Patterson

Oral Presentation

360 In-situ TEM study of ice nucleation and growth

Lifen Wang¹

¹Institute of Physics, Chinese Academy of Sciences, Zhongguancun, China

461 Investigating stability of ZIF-8 metal organic framework in operational environments: potential candidate for host-guest chemistry

Pritam Banerjee¹, Roland Fischer², Kathrin Kollmannsberger², Joerg Jinschek¹

¹National Centre for Nano Fabrication and Characterisation, Technical University of Denmark, Fysikvej 307, Denmark, ²Catalysis Research Centre and Department of Chemistry, Technical University of Munich, Lichtenbergstr. 4, Germany

528 Fine-tuning the Size of ZIF-L Nanosheets Through Controlled Synthesis

Sara Talebi Deylamani¹, Dr. Giuseppe Di Palma¹, Dr. Pritam Banerjee¹, Prof. Kasper S. Pedersen², Prof. Joerg R. Jinschek¹

¹DTU Nanolab, Technical University of Denmark (DTU), Lyngby, , Denmark, ²DTU Chemistry, Technical University of Denmark (DTU), Lyngby, , Denmark

1070 Visualizing atomic structure of novel three-dimensional covalent organic frameworks by 3DED and high-resolution (S)TEM

Jia Lyu¹, Yaozu Liu², Professor Qianrong Fang², Professor Xiaodong Zou¹, Researcher Hongyi Xu¹, Professor Daliang Zhang³

¹Department of Materials and Environmental Chemistry, Stockholm University, Stockholm, Sweden, ²State Key Laboratory of Inorganic Synthesis and Preparative Chemistry, Jilin University, Changchun, P. R. China, ³Multi-Scale Porous Materials Center, Institute of Advanced Interdisciplinary Studies & School of Chemistry and Chemical Engineering, Chongqing University, Chongqing, P. R. China

80 Ptychographic X-ray computed tomography of porous membranes with nanoscale resolution

Dr. Radoslaw Gorecki^{1,2}, Carla C. Polo³, Tiago A. Kalile³, Eduardo X. S. Miqueles³, Yuri R. Tonin³, Lakshmeesha Upadhyaya^{1,2}, Florian Meneau^{3,4}, Suzana P. Nunes^{1,2,5}

¹Environmental Science and Engineering Program, Biological and Environmental Science and Engineering, King Abdullah University of Science and Technology (KAUST), KAUST, Thuwal, Saudi Arabia, ²Advanced Membranes and Porous Materials Center, King Abdullah University of Science and Technology (KAUST), KAUST, Thuwal, Saudi Arabia, ³Brazilian Synchrotron Light Laboratory (LNLS), Brazilian Center for Research in Energy and Materials (CNPEM), Campinas, Brazil, ⁴Institute of Chemistry, University of Campinas (UNICAMP), Campinas, Brazil, ⁵Chemistry and Chemical Engineering Programs, Physical Science and Engineering, King Abdullah University of Science and Technology (KAUST), KAUST, Thuwal, Saudi Arabia

131 Understanding Twinning and Hierarchical Structure of Synthetic Guanine with 4D-Scanning Transmission Electron Microscopy

Rebekka Klemmt¹, Christian Lund Rasmussen¹, Ass. Prof. Espen Draht Bøjesen¹, Prof. Henrik Birkedal¹

¹Interdisciplinary Nanoscience Center (iNANO), Aarhus University, Aarhus, Denmark

466 Unveiling the three-dimensional ultrastructure of Poly Lactic Acid (PLA) spherulites by means of electron microscopy

Dr Paola Parlanti¹, Dr Giovanna Molinari², Prof Andrea Lazzeri^{3,4}, Dr Mauro Gemmi¹

¹Istituto Italiano di Tecnologia CMI-IIT, Pontedera, Italy, ²National Research Council CNR-IPCF, Pisa, Italy, ³University of Pisa, Pisa, Italy, ⁴National Interuniversity Consortium of Materials Science and Technology, Florence, Italy

520 Scanning electron diffraction reveals the molecular ordering of polysaccharides at the nanoscale
Mr. Mathias Nero¹, Dr. Tom Willhammar¹

¹Stockholm University, Stockholm, Sweden

526 Cryogenic electron microscopy for native state analysis of soft- and nano-materials

Dario Luis Fernandez Ainaga¹, Teresa Roncal-Herrero¹, Martha Ilett¹, Stuart Micklethwaite¹, Zabeada Aslam¹, Eleena Naveed¹, James Hitchcock¹, Cheng Cheng¹, Benjamin Lobel¹, Olivier Cayre¹, Dr Nicole Hondow¹

¹University of Leeds, Leeds, UK

693 Investigating the chemical oxidative polymerization of 1,8 - dihydroxynaphthalene using a correlative in-situ approach

Dr Nivedita Sudheer^{1,2}, Kevin Ziegler³, Emmanuel Maisonhaute⁴, Vincent Ball³, Cédric Boissière⁵, Tom Ferte², Dris Ihiawakrim², Clement Sanchez^{1,5}, Ovidiu Ersen²

¹Collège de France, Paris, France, ²Institut de physique et chimie des Matériaux de Strasbourg (IPCMS), Strasbourg, France, ³Institut national de la santé et de la recherche médicale (INSERM), Strasbourg, France, ⁴Laboratoire Interfaces et Systèmes Electrochimiques (LISE), Paris, France,

⁵Laboratoire de Chimie de la Matière Condensée de Paris (LCMCP), Paris, France

Poster Presentation

28 Examination of the Thermal and Morphological properties of Spartium Junceum Fibers for Flame Retardant Purposes

Zorana Kovacevic¹, Mrs. Lucia Spasevski², Prof.Dr. SANDRA BISCHOF¹

¹University of Zagreb Faculty of Textile Technology, Zagreb, Croatia, ²Oxford Instruments NanoAnalysis, High Wycombe, United Kingdom

44 TRIBLOCK POLY(2-OXAZOLINE)S WITH A FLUORINATED BLOCK AS A NEW PLATFORM FOR ADVANCED SELF-ASSEMBLY: CRYO-TEM STUDY

Sergey Filippov¹, Dr. Leonid Kaberov², Dr. Lubomir Kovacic³, Prof. Richard Hoogenboom⁴

¹DWI Institute of Interactive Materials, Aachen, Germany, ²Friedrich Schiller University, Jena, Germany, ³C-CINA, Biozentrum, University of Basel, Basel, Switzerland, ⁴Ghent University, Ghent, Belgium

53 Optimizing micrograph contrast in multicomponent systems at low-voltage scanning electron microscopy

Asia Matatyaho Ya'akobi¹, Irina Davidovich¹, Yeshayahu Talmon¹

¹The Department of Chemical Engineering and The Russell Berrie Nanotechnology Institute (RBNI), Haifa, Israel

86 A Secondary Electron Hyperspectral Imaging characterisation of mechanochemically functionalised carbon black materials

James Nohl^{1,2}, Nicholas Farr¹, Maria Rosaria Acocella³, Serena Cussen⁴, Cornelia Rodenburg¹

¹Department of Materials Science and Engineering, The University of Sheffield, Mappin Street, Sheffield, UK, ²The Faraday Institution, Quad One, Becquerel Avenue, Harwell Campus, Didcot, UK,

³Department of Chemistry and Biology "A. Zambelli", University of Salerno, Via Giovanni Paolo II, 132- 84084 Fisciano, Italy, ⁴School of Chemistry, University College Dublin, Belfield, Dublin 4, Ireland

153 Probing chemical pathways in polymer membranes despite electron beam damage

Dr Catriona M. McGilvery¹, Dr Patricia Abellan², Prof Quentin M. Ramasse³, Prof Alexandra E. Porter¹

¹Imperial College London, London, UK, ²CNRS-Nantes University, Nantes, France, ³SuperSTEM Laboratory, Daresbury, UK

407 Towards advanced polymer membranes for hydrogen technologies through dose-optimised Focused Ion Beams

Dr Ofentse Makgae¹, Dr Martha Briceno de Gutierrez¹

¹Johnson Matthey Technology Centre, Reading, United Kingdom

473 4D-STEM and EELS Analysis of Complex C-based Sensor Architectures

Mr Charles Otieno Ogolla¹, Mr Charles Otieno Ogolla¹, Mr Marco Hepp¹, Prof. Benjamin Butz¹, Tristan Zemke

¹University of Siegen, Siegen, Germany

490 Elucidating functionalities of N-doped carbonaceous materials by means of in-situ TEM

Dr Nadezda Tarakina¹, Dr. Diana Piankova¹, Dr. Hannes Zschiesche¹, Dr. Jing Hou¹, Prof. Dr. Markus Antonietti¹

¹Department of Colloid Chemistry, Max Planck Institute of Colloids and Interfaces, Potsdam, Germany

576 Cryogenic large volume 3D and TEM sample preparation with multiple ion species plasma FIB

Dr. Min Wu, Haifeng Gao, Devin Wu

¹Thermo Fisher Scientific, Eindhoven, The Netherlands

766 Solvent-induced softening of polymethyl methacrylate surfaces

Dr James Bowen¹, Dr Simon Collinson

¹The Open University, Milton Keynes, UK

908 Cellulose-based Nanocomposites for Sensor Applications: Characterization and Performance Evaluation

Asst. Prof. Domagoj Belić¹, Assoc. Prof. Mislav Mustapić¹, M.Sc. Dino Galić¹, B.Sc. Barbara Špigl¹, B.Sc. Sara Stivi¹, Assoc. Prof. Željko Skoko², Ph.D. Teodoro Klaser³, Assoc. Prof. Md Shahriar Al Hossain⁴

¹Department of Physics, J. J. Strossmayer University of Osijek, Osijek, Croatia, ²Department of Physics, Faculty of Science, University of Zagreb, Zagreb, Croatia, ³Ruđer Bošković Institute, Zagreb, Croatia, ⁴Faculty of Engineering, Architecture and Information Technology, The University of Queensland, Brisbane, Australia

1021

Morphological characterization of the electric field aligned block copolymers containing liquid crystal moiety

Monika Król¹, Isaac Álvarez Moisés², Janne Ruokolainen¹, Jean-François Gohy²

¹Aalto University, Espoo, Finland, ²Université catholique de Louvain, Louvain-la-Neuve, Belgium

1047 Cryo-EM as a tool for observing alginate-based hydrogels

Katerina Mrazova^{1,2}, Anna Havlickova², Diana Cernayova², Kamila Hrubanova¹, Petr Sedlacek², Vladislav Krzyzaneck¹

¹Institute of Scientific Instruments of the CAS, v. v. i., Brno, Czech Republic, ²Faculty of Chemistry, Brno University of Technology, Brno, Czech Republic

1081 Analysis of the local chain orientation in conjugated polymer films

Mr Timothy Lambden¹, Dr Joonatan Laulainen¹, Dr Maximilian Moser², Dr Christina Kousseff², Professor Iain McCulloch^{2,3}, Dr Scott Keene^{4,5}, Professor Paul Midgley¹

¹Department of Materials Sciences and Metallurgy, University of Cambridge,, Cambridge, United Kingdom, ²Department of Chemistry, Chemistry Research Laboratory, University of Oxford, Oxford, United Kingdom, ³Department of Electrical and Computer Engineering, Engineering Quadrangle, 41 Olden Street, Princeton, USA, ⁴Electrical Engineering Division, Department of Engineering, University of Cambridge, Cambridge, UK, ⁵Cavendish Laboratory, University of Cambridge, , Cambridge, UK

Late Poster Presentation

1175 In-situ liquid-cell dynamic TEM observations of liquid crystal nanocomposite phase transitions

Ms Olga Kaczmarczyk¹, Katarzyna Matczyszyn¹, Andrzej Żak¹

¹Institute of Advanced Materials, Faculty of Chemistry, Wrocław University of Science and Technology, Wrocław, Poland

1231 Self-assembled nanoparticles in a thin film of water

Dr Crispin Hetherington¹, Dr Dmitry Baranov², Dr Katarzyna Makasewicz³

¹nCHREM, Lund University, Lund, Sweden, ²Chemical Physics and NanoLund, Lund University, Lund, Sweden, ³Institute for Chemical and Bioengineering, ETH Zürich, Zürich, Switzerland

1322 Electron Energy-Loss Spectroscopy of Liquids

Sofie Tidemand-Lichtenberg¹, Shima Kadkhodazadeh¹, Kristian Speranza Mølhav¹

¹Technical University of Denmark, Kgs. Lyngby, Denmark

1187

Probing the structure and dynamics of active molecular materials with cryo and liquid EM

Professor Joe Patterson

PS-07 (2), Plenary, august 30, 2024, 10:30 - 12:30

360

In-situ TEM study of ice nucleation and growth

Lifen Wang¹

¹Institute of Physics, Chinese Academy of Sciences, Zhongguancun, China

PS-07 (1), Plenary, August 29, 2024, 15:00 - 16:00

Ice is one of the most omnipresent solids on Earth, yet its crystallization is not fully understood. In particular, a long-standing debate is whether natural ice can form in a metastable pure-cubic phase. A mainstream view attributes the divergence to the stacking disordered ice (I_{sd}) with a mixture of cubic and hexagonal sequences that preferentially nucleate and grow at low temperatures typically under 200 K, where complex kinetics in ice crystallization has also defied understanding thus far. This is due to that the direct and reliable determination of the structure of metastable ice requires ultra-high spatiotemporal resolution in an in-situ freezing environment, which remains a major outstanding challenge in the community. Here, through developing the in-situ cryogenic TEM, we directly tracked and unveiled the heterogeneous polymorphic ice nucleation and crystallization with molecular resolution during the water vapor deposition process at 102 K. We further pinpointed the atomic structure of polymorphic ice crystallites and identified distorted ice tetrahedral configurations as crystal defects with molecular resolution, which were not accessible before. Employing the electron beam as both the imaging probe and activation source, we were able to trigger and consequently monitor the kinetic transition process of stacking disordered ice (I_{sd}) to ice I_c, demonstrating the unexpected meta-stability of ice I_{sd} with respect to ice I_c. Our measurements shed new light on the structure and dynamics process determined heterogeneous nucleation of polymorphic ice. While a deep understanding of ice crystallization requires microscopic details, our realization of direct real-space imaging of growing ice crystallites at the molecular level is a key step towards reconciling experimental and theoretical investigations into the structure, nucleation, and crystallization based complex phenomena in ice family and polymorphic crystals.

Keywords:

Ice, In-situ TEM, polymorphism, Crystallization

Reference:

- 1 Huang, X. et al. Tracking cubic ice at molecular resolution. *Nature* 617, 86-91, doi:10.1038/s41586-023-05864-5 (2023).
- 2 Wang, L. et al. Microscopic Kinetics Pathway of Salt Crystallization in Graphene Nanocapillaries. *Physical Review Letters* 126, 136001, doi:10.1103/PhysRevLett.126.136001 (2021).
- 3 Wang, L. et al. Synthesis of Honeycomb-Structured Beryllium Oxide via Graphene Liquid Cells. *Angewandte Chemie International Edition* 59, 15734-15740, doi:https://doi.org/10.1002/anie.202007244 (2020).
- 4 Zhu, L. et al. Visualizing Anisotropic Oxygen Diffusion in Ceria under Activated Conditions. *Physical Review Letters* 124, 056002, doi:10.1103/PhysRevLett.124.056002 (2020).

461

Investigating stability of ZIF-8 metal organic framework in operational environments: potential candidate for host-guest chemistry

Pritam Banerjee¹, Roland Fischer², Kathrin Kollmannsberger², Joerg Jinschek¹

¹National Centre for Nano Fabrication and Characterisation, Technical University of Denmark, Fysikvej 307, Denmark, ²Catalysis Research Centre and Department of Chemistry, Technical University of Munich, Lichtenbergstr. 4, Germany

PS-07 (1), Plenary, August 29, 2024, 15:00 - 16:00

Background incl. aims

Ultra-small atom precise metal nanoclusters (NCs) have emerged as (electro)catalysts due to their large surface area and abundant unsaturated active sites. However, surface ligands and strong agglomeration tendency limit NCs' catalytic activity [1]. Zeolitic imidazolate frameworks (ZIFs), a subset of metal-organic-frameworks (MOFs) emerge as excellent support to host NCs due to their well-controllable pore size of 11.6 Å, pore aperture 3.4 Å and high internal surface area. Understanding the state and the stability of these NCs inside the ZIF pores under operating condition is crucial for tuning the catalytic properties.

Generally, in high-resolution TEM (HRTEM) experiments few atom NCs appear to be more stable than ZIF when exposed to the electron beam. The atomicity of Pt NCs is measured using spectroscopy techniques as mentioned [2]. Therefore, HRTEM experiments to understand the structure, e.g. of Pt₂₇@ZIF-8 nanocomposites (shown in fig. 1(a)), are very challenging because ZIF-8 tends to lose crystallinity already at a cumulative electron dose of $\sim 25 \text{ e-}\text{\AA}^{-2}$, which is far below the required dose for standard high-resolution images [3]. So far, no quantitative measurement of a critical electron dose limit for real-time observations of ZIF-8 (and NCs@ZIF-8) under operating conditions (elevated temperature and various gaseous environments) has been reported. Hence, the structural and morphological integrity in such experiments as well as the mechanism of possible loss of crystallinity under the exposure of electron beam are still largely unexplored. However, we consider this to be a prerequisite before conducting an (in-situ) study of such a beam sensitive material.

Methods

To establish the critical electron dose for ZIF-8, we systematically investigated here the effect of the accumulated electron dose on the ZIF-8 crystallinity using selected area diffraction (SAD). Thereby we quantitatively measured 1. the fading of intensity of specific Bragg planes as well as 2. the relative displacement of Bragg planes, both as a function of accumulated total electron dose. We have varied the TEM sample support (graphene versus amorphous holey carbon) and we have applied different TEM imaging parameters such as accelerating voltage (200 vs 300 keV) as well as electron dose rates (0.33, 0.5, 1, and 2 $\text{e-}\text{\AA}^{-2}\text{s}^{-1}$). The bright field (BF) image and the corresponding SAD pattern of single crystalline ZIF-8 particles are shown in fig. 1(b, c). The fading of the relative intensity of 431 Bragg ring in the SAD pattern as function of cumulative dose is shown in fig. 1(d).

Further, we investigated the stability of ZIF-8 at different sample temperatures, varying the temperature from -176°C to 550°C . Both the TEM cryo and heating experiments were performed in a ThermoFisher Titan microscope using a Gatan 626 and Inconel holder, respectively. In the heating experiment the temperature was varied from 200 to 550°C with a step of 50°C .

Under all experimental conditions, the critical accumulated dose was determined by measuring the fading of the respected Bragg spots. In order to understand the mechanism of loss in crystallinity we further measure any crystal lattice expansion or shrinkage indicated by changes in the radius of the SAD rings (= Bragg planes).

At last, we investigated the stability of ZIF-8 under oxygen atmosphere and elevated temperatures, using a ThermoFisher Titan ETEM (300 keV) and a Gatan Inconel heating holder. The temperature was varied from 350°C to 550°C under constant O₂ pressure of 2.7 mbar. Again, the transformation

of ZIF-8 to ZnO nanoparticles was observed in BF images and SAD pattern, and the change in the crystal structure and morphology of the particles were studied.

Results

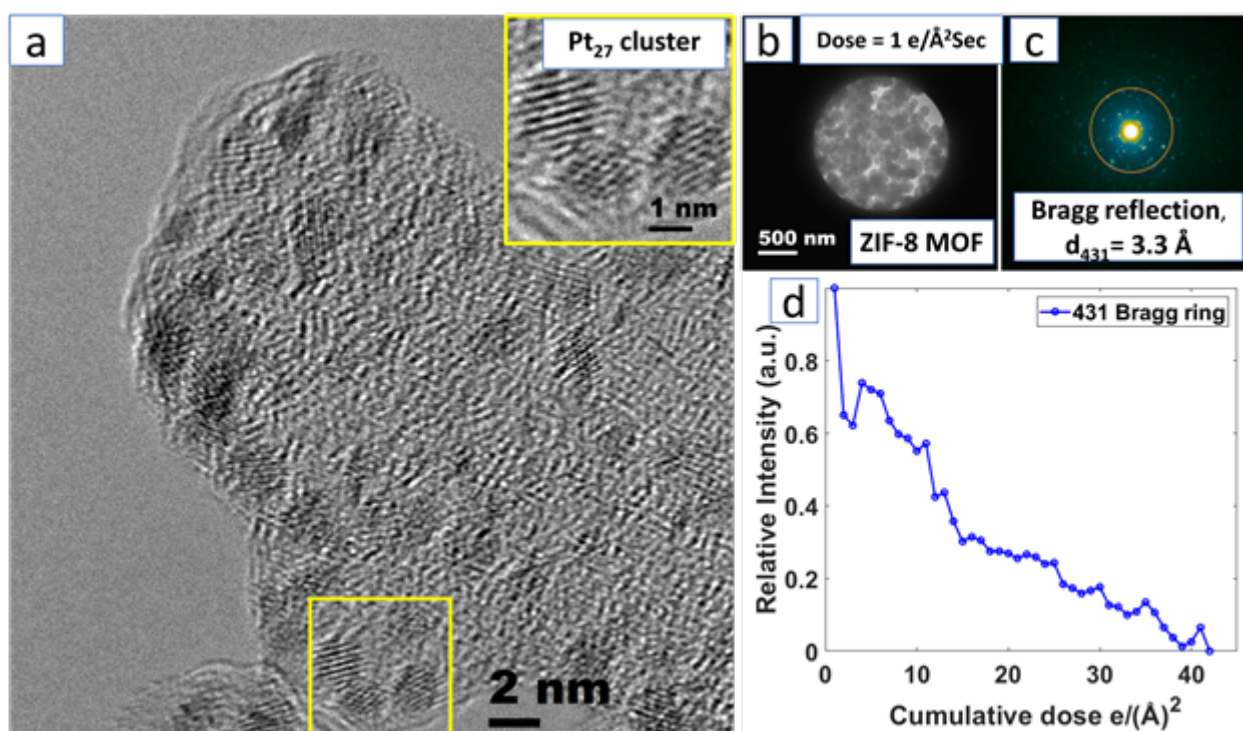
Based on our systematic study, we report the critical limit of cumulative dose of $\sim 10 \text{ e}^{-}\text{\AA}^{-2}$ to enable non-invasive structural characterization using HRTEM imaging. We thereby provide insights into the fundamental mechanisms of electron beam-induced damage in ZIF-8.

The influence of different imaging conditions, substrate materials and temperature on the critical dose will be discussed. Finally, the challenges and development of in-situ gas experiments on beam-sensitive materials will be discussed, taking ZIF-8 MOF to ZnO transformation as a reference.

Conclusion

This work provides a deeper understanding of the interaction of electrons with MOF (here: ZIF-8) under different HRTEM imaging conditions, an understanding of the underlying damage mechanism and the identification of optimal conditions for (in-situ) characterization experiments.

These findings have significant implications for the further development of NC@MOF nanocomposites in a wide range of applications, such as catalysis.



Keywords:

Nanoclusters, metal-organic-framework, HRTEM, ETEM, In-situ-TEM

Reference:

- [1] K. L. Kollmannsberger, L. Kronthaler, J. R. Jinschek, and R. A. Fischer, "Defined metal atom aggregates precisely incorporated into metal-organic frameworks," *Chem. Soc. Rev.*, vol. 51, no. 24, pp. 9933–9959, 2022.
- [2] K. L. Kollmannsberger, "Defined guest-MOF systems toward tailored catalysts" 2023.
- [3] Y. Zhu et al., "Unravelling surface and interfacial structures of a metal-organic framework by transmission electron microscopy," *Nat. Mater.*, vol. 16, no. 5, pp. 532–536, 2017.

528

Fine-tuning the Size of ZIF-L Nanosheets Through Controlled Synthesis

Sara Talebi Deylamani¹, Dr. Giuseppe Di Palma¹, Dr. Pritam Banerjee¹, Prof. Kasper S. Pedersen², Prof. Joerg R. Jinschek¹

¹DTU Nanolab, Technical University of Denmark (DTU), Lyngby, , Denmark, ²DTU Chemistry, Technical University of Denmark (DTU), Lyngby, , Denmark

PS-07 (1), Plenary, august 29, 2024, 15:00 - 16:00

Background incl. aims

To design novel hierarchical nanostructures with predefined properties and functionalities, e.g. for engineering and nanomedicine applications, we need to understand their bottom-up assembly processes as well as inherent structure-property relationships. This will open opportunities for precise synthesis of nanomaterials with targeted functionalities by simply controlling property-related structural characteristics in the bottom-up synthesis process, i.e. controlling size, morphology, crystallinity, etc. [1].

In this context, metal-organic frameworks (MOFs) have emerged as a customizable hierarchical material known for their high chemical and thermal stability. Controlled synthesis of these highly porous crystalline material is primarily about precise control of their chemistry, size, shape, and crystallinity. And, this ability has already been demonstrated, leading to controlled design of MOF structures with well-defined properties for various applications, such as gas storage & separation, wastewater treatment, and catalysis [2] [3]. For example, in catalysis applications where enhancing access of reactants to active sites is crucial, it is advantageous to design MOF nanosheets with precisely controlled thickness, as they offer a larger external surface area and decreased diffusion resistance [4].

Here, we investigate the synthesis process of zeolitic imidazolate frameworks (ZIF) with a leaf-like shape (ZIF-L nanosheets) to understand whether and how precisely we can control the nanosheet thickness (i.e. controlling the surface-to-volume ratio). We apply a series of photon- and electron-based characterization methods to understand the nucleation processes and growth mechanisms of ZIF-L nanosheets.

Methods

The ZIF-L nanosheets were prepared using a standard bottom-up synthesis method in which the synthesis parameters, including ligand-to-metal ratio, selection of additional ligands (modulators) as well as reaction time were systematically varied to synthesize uniformly thin nanosheets with controlled thickness.

A detailed structural characterization was conducted. Fourier-transform infrared spectroscopy (FTIR), scanning electron microscope (SEM), and X-ray diffraction (XRD) were used to confirm that ZIF-L was successfully synthesized. Crystallinity of the nanosheets was further determined by electron diffraction (ED). The size of the ZIF-L nanosheets (thickness and surface area) was determined using SEM and transmission electron microscopy (TEM).

ZIF-L are extremely sensitive to electron beams (critical dose $\ll 100$ e-/Å²). Therefore, all TEM experiments were performed under low-dose conditions and/or using a Gatan cryo sample holder (cryo-TEM).

Results

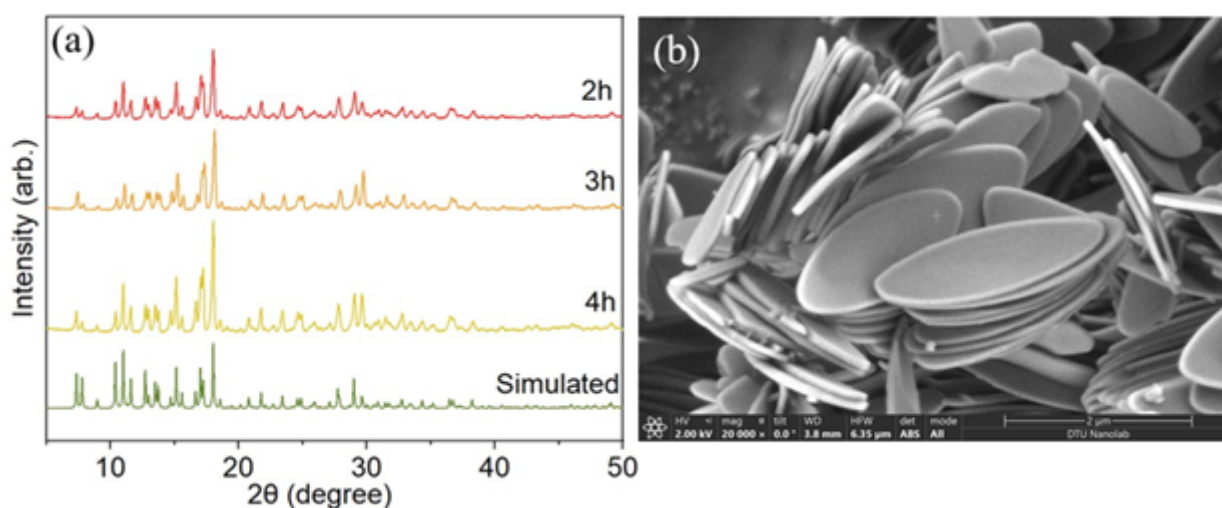
ZIF-L nanosheets were synthesized by systematically varying the synthesis parameters to control their thicknesses. When the synthesis time was reduced from 4 hours to 2 hours at a constant ligand-to-metal ratio of <6 , the nanosheet thickness decreased from ~ 135 nm to ~ 95 nm, as measured by SEM and TEM images. FTIR spectra, XRD as well as ED patterns confirmed that all nanosheets were

ZIF-L single crystals. By further reducing the synthesis time to 20 minutes [5], the crystal thickness was further decreased to well below 90 nm. However, not all crystals exhibited nanosheet shapes. The particles showed nonuniform thickness and were agglomerated into flower-like shapes. Therefore, modulator ligands in various concentrations were added in the synthesis process to precisely control the balance between nucleation process and crystal growth. SEM imaging confirms that the addition of a modulator ligand resulted in formation of well-defined thin ZIF-L nanosheets even at low reaction times. Further (cryo) TEM experiments were performed to understand details of the ZIF-L growth kinetics.

Conclusion

The precise control of the morphology of a particular nanosheet MOF presented here is a great example of a promising strategy for designing nanostructures with predefined functionalities from the bottom up.

In detail, we provide an approach to design ZIF-L nanosheets with controllable size (i.e. thickness). The synthesis time as well as the concentration of modulator ligands were varied systematically. Their effects on nucleation, crystal formation, crystal growth, and the final leaf-like morphology were investigated by a detailed characterization study.



Keywords:

Metal-organic frameworks, nanosheets, FTIR, TEM

Reference:

1. Liu, M., Zu, L., & Hudson, Z. M. (2022). Mechanistic Principles for Engineering Hierarchical Porous Metal–Organic Frameworks. *ACS nano*, 16(9), 13573-13594.
2. Furukawa, H., Cordova, K. E., O’Keeffe, M., & Yaghi, O. M. (2013). The chemistry and applications of metal-organic frameworks. *Science*, 341(6149), 1230444.
3. Zhang, J., Cheng, N., & Ge, B. (2022). Characterization of metal-organic frameworks by transmission electron microscopy. *Advances in Physics: X*, 7(1), 2046157.
4. Li, H., Hou, J., Bennett, T. D., Liu, J., & Zhang, Y. (2019). Templated growth of vertically aligned 2D metal–organic framework nanosheets. *Journal of materials chemistry A*, 7(10), 5811-5818.
5. Mor, J., Utpalla, P., Kumar, R., Bahadur, J., & Sharma, S. K. (2023). Evolution of Local Structure and Pore Architecture during Zeolitic Imidazolate Framework-L to Zeolitic Imidazolate Framework-8 Phase Transformation Investigated Using Raman, Extended X-ray Absorption, and Positron Annihilation Lifetime Spectroscopy. *Chemistry of Materials*, 35(17), 6625-6636.

1070

Visualizing atomic structure of novel three-dimensional covalent organic frameworks by 3DED and high-resolution (S)TEM

Jia Lyu¹, Yaozu Liu², Professor Qianrong Fang², Professor Xiaodong Zou¹, Researcher Hongyi Xu¹, Professor Daliang Zhang³

¹Department of Materials and Environmental Chemistry, Stockholm University, Stockholm, Sweden,

²State Key Laboratory of Inorganic Synthesis and Preparative Chemistry, Jilin University, Changchun, P. R. China, ³Multi-Scale Porous Materials Center, Institute of Advanced Interdisciplinary Studies & School of Chemistry and Chemical Engineering, Chongqing University, Chongqing, P. R. China

PS-07 (1), Plenary, august 29, 2024, 15:00 - 16:00

Covalent organic frameworks (COFs) are a family of porous materials constructed through organic blocks connected by covalent bonds. Its versatility of functionality, its well-defined pores, and its high surface area / high porosity have cultivated many applications in gas storage, catalysis, and separation areas.

Determining the structure of three-dimensional COFs is important for understanding their structure-function relationships and enables the rational design of materials with better performance. The most trivial way to gather the structure information is through the single-crystal X-ray diffraction (SCXRD) method. However, the small crystal sizes of the COFs hindered the common routine of *ab initio* structure solution. Additionally, the poor crystallinity and polymorphism of COFs also make them difficult to analyze using powder XRD data.

Electron microscopy is widely used for structure characterization in material science and gained great success on the elucidation of many complex structures. It can investigate bulk structures of small crystals by three-dimensional electron diffraction (3DED) technique and local structures by imaging. Acquiring atomic-resolution images on 3D COFs remains challenging, especially due to the electron beam damage. In recent years, the development of electron detectors and image-acquisition methods have enabled high-resolution (S)TEM with ultralow electron doses, largely overcoming this challenge. The poor crystallinity, disorders, guest molecules, and flexible characteristics of COFs still undermine the determination of the COFs' structure.

We use the 3DED technique under cryogenic conditions to get the averaging atomic structure of novel 3D COFs. The accumulated electron dose is $6\sim 15\text{ e}^-/\text{\AA}^2$. The structure is validated with corresponding low-dose high-resolution electron microscopy (HREM) images with relatively low position offsets. We hope this investigation will cultivate the further development of structure-solving on COFs and other organic materials.

Keywords:

3DED, Low-dose HREM, 3D COFs

Reference:

1. J. Am. Chem. Soc. 2021, 143, 4, 2123–2129.
2. J. Am. Chem. Soc. 2023, 145, 17, 9679–9685.
3. Zeitschrift für Kristallographie, 2010, 225, 2-3, 94-102.
4. Acc. Mater. Res. 2022, 3, 5, 552–564.
5. Science, 2018, 359, 675-679.

Ptychographic X-ray computed tomography of porous membranes with nanoscale resolution

Dr. Radoslaw Gorecki^{1,2}, Carla C. Polo³, Tiago A. Kalile³, Eduardo X. S. Miqueles³, Yuri R. Tonin³, Lakshmeesha Upadhyaya^{1,2}, Florian Meneau^{3,4}, Suzana P. Nunes^{1,2,5}

¹Environmental Science and Engineering Program, Biological and Environmental Science and Engineering, King Abdullah University of Science and Technology (KAUST), KAUST, Thuwal, Saudi Arabia, ²Advanced Membranes and Porous Materials Center, King Abdullah University of Science and Technology (KAUST), KAUST, Thuwal, Saudi Arabia, ³Brazilian Synchrotron Light Laboratory (LNLS), Brazilian Center for Research in Energy and Materials (CNPEM), Campinas, Brazil, ⁴Institute of Chemistry, University of Campinas (UNICAMP), Campinas, Brazil, ⁵Chemistry and Chemical Engineering Programs, Physical Science and Engineering, King Abdullah University of Science and Technology (KAUST), KAUST, Thuwal, Saudi Arabia

PS-07 (2), Plenary, august 30, 2024, 10:30 - 12:30

Background Incl. Aims

3D images of porous materials in high resolution have been so far obtained using transmission electron tomography or focused ion beam coupled with scanning electron microscopy. These methods require ultra-vacuum conditions, and only a small volume of the sample is visualized. Here, we demonstrate the application of ptychographic x-ray computed tomography for visualizing soft matter with a resolution of 26 nm over large fields of view. We showcase the technique's capabilities by imaging polymer hollow fiber porous membranes.

Porous materials have essential functions in nature, whether for water and nutrient transport in plants and other biological systems or for the storage of oil and water in rock reservoirs. Synthetic polymeric materials are key for chromatography and membrane separation processes. Their application is well-established in water desalination, hemodialysis, gas separation, and is expanding in nanofiltration for chemical separations. The advantages of membrane technology are low energy requirement, and low carbon footprint combined with a compact design that allows packing a large membrane area within a small volume. Effective membranes have a complex porous structure to secure selectivity, mechanical stability, and fast transport characteristics. Porosity and interconnectivity determine the membrane performance.

Thanks to the high-penetration depth of the X-ray beam, we visualize the 3D complex porous structure of polyetherimide ultrafiltration hollow fibers in a non-destructive manner and obtain quantitative information about pore size distribution and pore network interconnectivity across the whole membrane wall. The non-destructive nature of this method, coupled with its ability to image samples without requiring modification or a high vacuum environment, makes it valuable in the fields of porous- and nano-material sciences, enabling imaging under different environmental conditions.

Methods

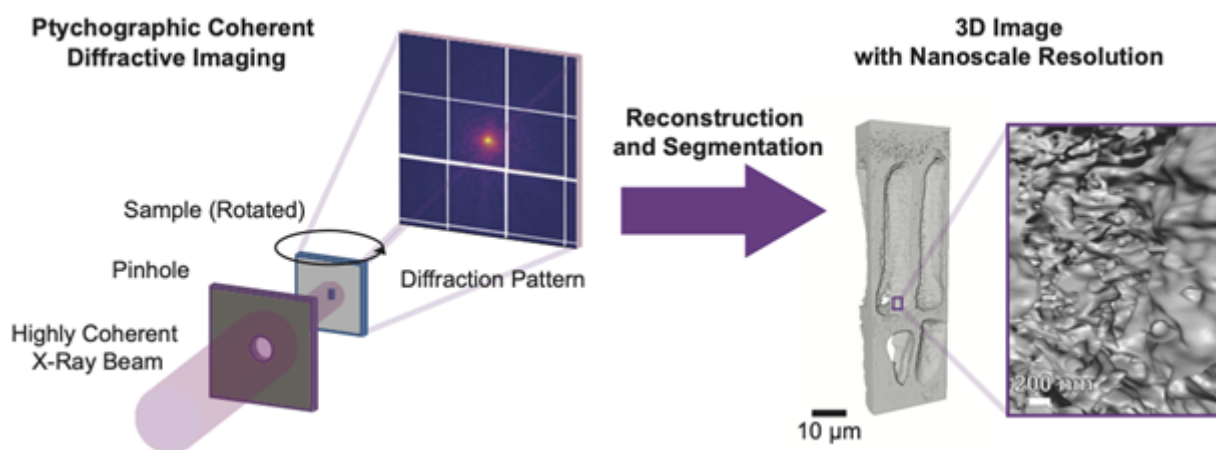
A highly coherent x-ray beam produced by SIRIUS, the 4th generation synchrotron source inaugurated in 2020 in Campinas, Sao Paulo, Brazil, was used at a dedicated beamline for x-ray imaging - Cateretê. Ptychographic x-ray computed tomography (PXCT) is a lensless coherent x-ray technique, where the specimen is raster scanned in two dimensions by a coherent x-ray beam defined by a pinhole, and diffraction patterns in the far-field are recorded at each position. The sample is rotated and the 2D scans are collected at different projections to obtain a 3D dataset for reconstructions.

Results

The high-performance computer reconstruction of the collected 2D projections resulted in detailed 3D images of the hollow fibers, with a resolution of 26 nm and a voxel size of 23 nm × 23 nm × 23 nm. Such a detailed model contains not only visual but also quantitative information, and it was used to evaluate the porosity gradient across the membrane walls for hollow fiber membranes. Apart from the porosity, we were able to study the evolution of the diameter size of every detected pore channel across the membrane thickness within the resolution limits (26 nm diameter), to evaluate the pore size distribution and changes across the entire membrane. We could also provide a comprehensive analysis of the interconnectivity of the pores.

Conclusions

The highly coherent X-ray beam generated by the 4th generation synchrotron source allows for the non-destructive analysis via PXCT with nanoscale resolution. The reconstruction of the X-ray coherent diffraction patterns from different projection angles, not only facilitated the visualization of complex porous morphology throughout the entire membrane wall volume but also provided a detailed 3D quantitative model of the porous network. The presented PXCT method is not limited to the measurements of porous structures but can be employed for resolving the nanostructure details in large samples within soft matter. Furthermore, thanks to the high-penetration depth of X-rays, PXCT allows for the analysis of the samples where the sectioning for electron microscopy methods is not feasible. The lack of vacuum requirements and the absence of sample modification, such as heavy metal staining, enable in situ analysis of samples in different environmental conditions. These advantages, coupled with the non-destructive nature of this technique, make it highly applicable in material science and biology for the understanding of complex porous- and nanomaterials offering nanometer-scale resolutions for large sample volumes and providing valuable quantitative information.



Keywords:

X-Ray Tomography, Ptychography, Polymer Membrane

Reference:

Górecki, R.; Polo, C.C; Kalile, T.A.; Miqueles, E.X.S.; Tonin, Y.R.; Upadhyaya, L.; Meneau, F.; Nunes, S.P., Ptychographic X-ray computed tomography of porous membranes with nanoscale resolution, *Communications Materials*, 4, 68, 2023

131

Understanding Twinning and Hierarchical Structure of Synthetic Guanine with 4D-Scanning Transmission Electron Microscopy

Rebekka Klemmt¹, Christian Lund Rasmussen¹, Ass. Prof. Espen Draht Bøjesen¹, Prof. Henrik Birkedal¹

¹Interdisciplinary Nanoscience Center (iNANO), Aarhus University, Aarhus, Denmark

PS-07 (2), Plenary, august 30, 2024, 10:30 - 12:30

Introduction:

Various biological systems can utilize guanine crystals in photonic structures. To synthesize structures of guanine that mimic these biological photonic systems, many factors of the crystallization need to be controlled, like the specific polymorphism, morphology, crystallographic lattice orientation, and the crystals' twinning. This requires new synthesis approaches, as well as novel characterization techniques. The possibility to acquire local crystallographic information by acquiring a whole diffraction pattern at each probed position in scanning transmission electron microscopy (STEM), a technique known as 4D-STEM, is thereby a promising technique to investigate twinning in more detail.

The aim of this study is to find synthesis approaches that can mimic guanine crystals utilized in biological photonic systems and link their properties to synthesis informed by their structure revealed by a combination of X-ray and state-of-the-art electron microscopy techniques.

Methods:

Guanine crystals were synthesized using a new synthesis approach using poly(diallyl dimethylammonium chloride) as an additive in solutions with pH levels of 13.

The resulting crystals were investigated with powder x-ray diffraction (PXRD), scanning electron microscopy (SEM), selected area electron diffraction (SAED), and 4D-STEM.

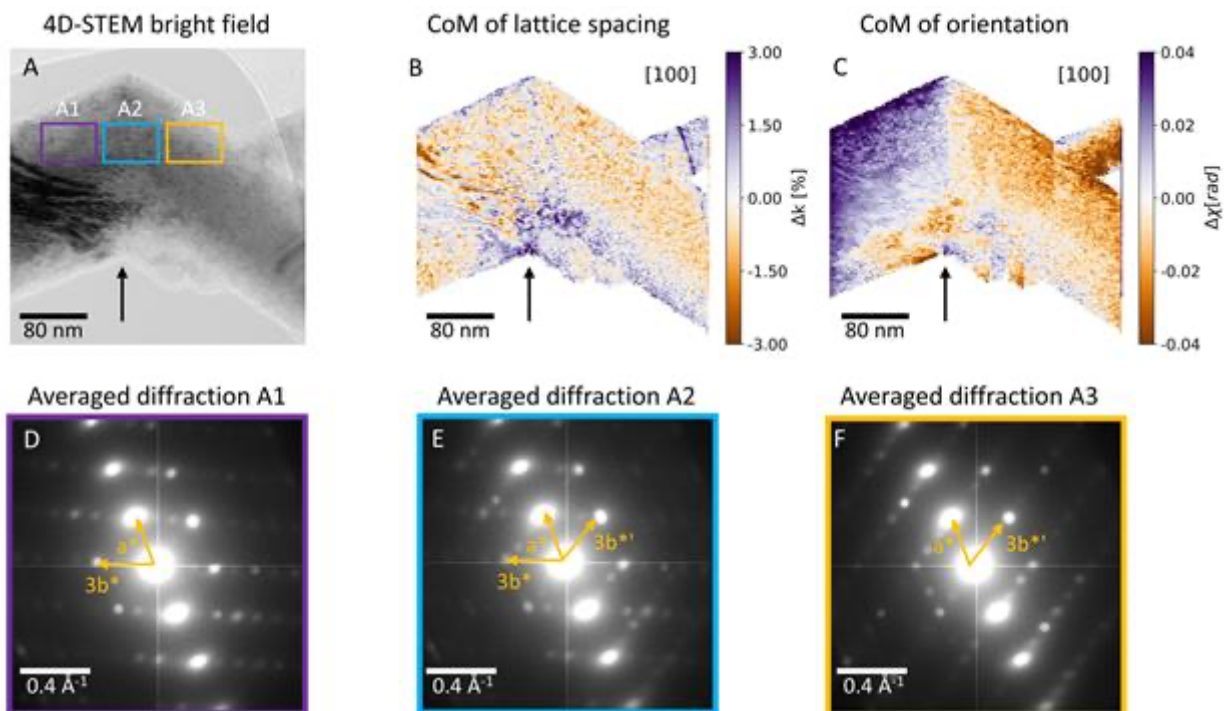
4D-STEM data was acquired at a low dose to avoid radiation damage to the guanine crystals. The resulting low signal-to-noise ratio made orientation mapping with commercially available programs challenging. Instead, the crystal orientation and lattice spacing changes were investigated with a center of mass (CoM) approach.

Results:

The synthesized guanine crystals adopted the same polymorph as those in biological photonic systems (β -guanine). They demonstrated flat and elongated structures, as also observed for crystals in biological photonic systems. Many crystals show kinks along their length, as exemplary pointed out by the arrow in the abstract figure. Via SAED, it was determined that these kinks coincided with twin boundaries in the crystals. Furthermore, diffuse scattering in the SAED pattern indicated disordered stacking of the guanine molecules. The novel CoM analysis of the 4D-STEM could relate the disordered stacking to smaller intergrown crystal domains. It indicated crystal growth by partly ordered granular nucleation. Such a growth of guanine was also observed in certain biological systems. From the CoM analysis, variations of the orientation and lattice spacing of the small crystal domains were mapped. Larger deviations from the averaged orientation and lattice spacing were found close to twinning boundaries, indicating strain minimization as the origin of twinning.

Conclusion:

The novel synthesis approach enabled tight synthesis control of guanine crystals with polymorph and morphology mimicking the polymorph and morphology found for crystals in biological photonic systems. The CoM analysis combined with an intricate understanding of the crystal structure and chemistry of guanine facilitated us to reveal otherwise inaccessible information about the crystal growth mechanism and origin of twinning in this, at first glance, seemingly simple yet biologically extremely relevant system. The study demonstrates the strength of employing 4D-STEM, informed by crystallographic knowledge for studies of bio-inspired complex materials systems.



Keywords:

synthetic guanine, 4D-STEM, twinning

466

Unveiling the three-dimensional ultrastructure of Poly Lactic Acid (PLA) spherulites by means of electron microscopy

Dr Paola Parlanti¹, Dr Giovanna Molinari², Prof Andrea Lazzeri^{3,4}, Dr Mauro Gemmi¹

¹Istituto Italiano di Tecnologia CMI-IIT, Pontedera, Italy, ²National Research Council CNR-IPCF, Pisa, Italy, ³University of Pisa, Pisa, Italy, ⁴National Interuniversity Consortium of Materials Science and Technology, Florence, Italy

PS-07 (2), Plenary, august 30, 2024, 10:30 - 12:30

Background incl. aims

Among biobased polymers, Poly Lactic Acid (PLA) is widely used in a variety of daily-use products from packaging to biomedicine, thanks to its properties (high strength, lightweight, toughness, corrosion resistance, transparency) and its ability to be easily and economically processed from renewable resources via traditional manufacturing techniques, such as injection-moulding. It is therefore a good candidate for replacing conventional petrochemical-derived plastics [1]. To improve the fabrication of this promising material, and optimize its properties (mechanical, thermal, etc.), a deeper comprehension of PLA morphology is mandatory. During the injection-moulding fabrication process, molten PLA solidifies into semicrystalline structures called “spherulites” (figure A), which are constituted by fibrillar lamellae (with thickness ranging from 10 to 30 nm), radially growing from a nucleation center (figure B). Depending on the manufacturing process, spherulites vary their morphology leading to a great impact on the macroscopic (e.g. mechanical) properties of this material [2]. To date, few studies extensively describe PLA spherulites’ morphology [3], but generally their characterization is limited to two-dimensional observations. Here we report our work in the three-dimensional (3D) investigation of PLA spherulites, by means of electron microscopy, toward a better comprehension of the relation between micro- and macroscopic properties of this material.

Methods

Dog-bone semicrystalline PLA samples were obtained by injection-moulding technique. PLA blocks (approx. 5 mm each side) were retrieved from the central portion of the dog-bone specimens, while keeping track of the orientation of the material within the hot mould. Then, using an ultramicrotome, we sectioned PLA blocks for transmission electron microscopy (TEM) imaging, by carrying out two different sectioning approaches: 1) directional sectioning; 2) serial sectioning. The first requires that the sample was cut into three mutually orthogonal directions, to investigate the PLA spherulites respective 3D arrangements in the block. The latter was instead chosen for 3D reconstruction of a single spherulite, by collecting sequential PLA sections, and imaging the same structure across the entire series of sections. We also performed scanning electron microscopy (SEM) imaging of the PLA sections collected on silicon wafers and tested the capabilities of focused ion beam scanning electron microscopy (FIB-SEM) for the spherulite volume imaging. Finally, ultramicrotome sectioning and FIB-SEM were used for fabricating PLA blocks suitable for X-ray ptycho-tomography.

Results

TEM analysis of directionally sectioned PLA blocks revealed the 3D organization of spherulites within the samples (figure A), which appeared to have an elliptical shape, with lower ellipticity extent at the faces perpendicular to the hot polymer flow direction during the injection-moulding processing. This would be directly related to the shear flow generated at the hot mould walls, which favored the elongation of the spherulites in the direction of the hot polymer flow.

Concerning the 3D characterization of a single spherulite, TEM imaging of the same structure across the entire series of sections collected with the serial sectioning approach allowed to reconstruct the lamellar arrangement within the spherulite, for a total volume of about 1.1 μm^3 (figure C).

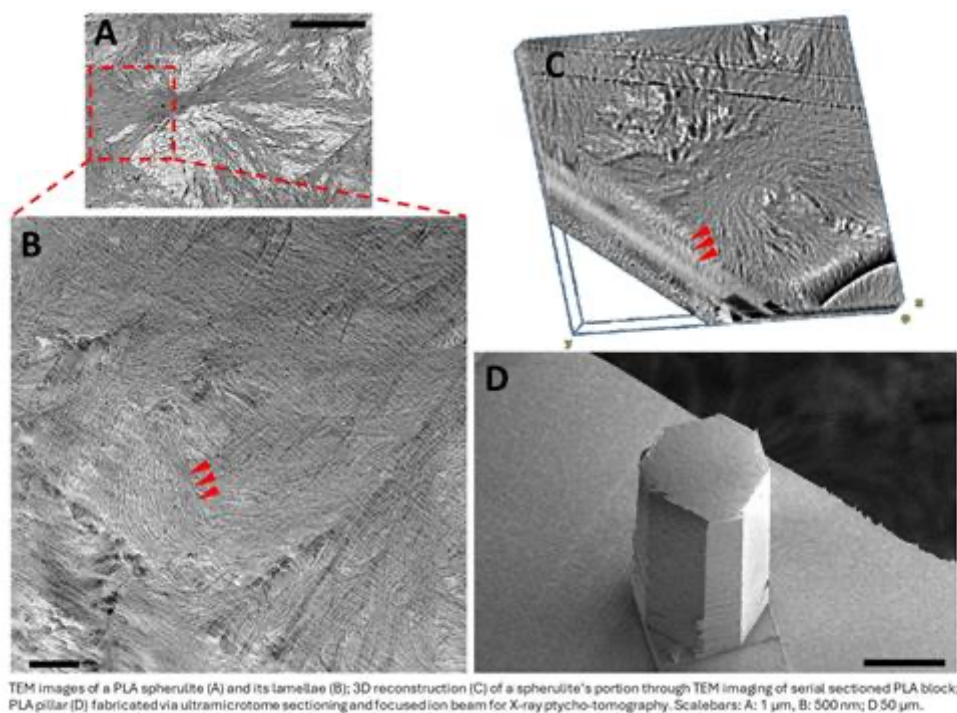
In order to reconstruct larger volumes of PLA spherulites, SEM analysis as well as FIB-SEM tomography were tested too, but spherulite's lamellae were not visible with the same resolution achieved with TEM.

For this reason, we are now approaching a new imaging technique (figure D): X-ray ptychotomography, pushed to the limit of spatial resolution (voxel side) down to tens of nanometers. This would give for the first time information along the third dimension about spherulites morphology and lamellar arrangements at the nanoscale.

Conclusion

PLA morphology and its mechanical/thermal characteristics are strictly related. Thus, the knowledge of PLA ultrastructure is particularly important for optimizing the fabrication process and finally obtaining a material with tailored macroscopic properties, such as thermal behavior, flexibility, strength. Our observations demonstrate the importance of microscopy in polymer science, through the application of cutting-edge (electron) microscopy techniques. Here we bring new insights of the PLA morphology, paving the route towards optimized industrial processing of this versatile and environmental friendly material.

The authors gratefully acknowledge support from the European Union's Horizon 2020 research and innovation program under the FET Open grant agreement 5DNanoPrinting - no. 899349.



Keywords:

Polymer, electron microscopy, three-dimension, ptychotomography

Reference:

- [1] S. Farah, D.G. Anderson, R. Langer. Physical and mechanical properties of PLA, and their functions in widespread applications — a comprehensive review. <https://doi.org/10.1016/j.addr.2016.06.012>
- [2] M. Safandowska, A. Rozanski. Ring-banded spherulites in polylactide and its blends. <https://doi.org/10.1016/j.polymertesting.2021.107230>
- [3] G. Molinari, P. Parlanti, L. Aliotta, A. Lazzeri, M. Gemmi. TEM morphological analysis of biopolymers: The case of Poly (Lactic Acid) (PLA). <https://doi.org/10.1016/j.mtcomm.2023.107868>

520

Scanning electron diffraction reveals the molecular ordering of polysaccharides at the nanoscale

Mr. Mathias Nero¹, Dr. Tom Willhammar¹¹Stockholm University, Stockholm, Sweden

PS-07 (2), Plenary, August 30, 2024, 10:30 - 12:30

Background

Cellulose is the most abundant biopolymer. Nature links glucan units to form polysaccharide chains which are organized in an intricate network of hydrogen bonds into crystalline cellulose fibers. These fibers are assembled into hierarchical structures that constitute the secondary cell wall of plants, forming the basis for their mechanical properties. The macroscopic attributes of these materials are determined by chemical interactions and mesoscopic organization spanning from the atomic scale to the macroscopic level. Understanding these assemblies is vital for grasping the properties of biological materials and for exploring ways to incorporate these naturally occurring components into hybrid materials.

Biopolymers are fundamentally challenging to study using electron microscopy due to their delicate and electron beam sensitive nature. Using scanning electron diffraction we can obtain unique nanoscale information about the molecular ordering of the polysaccharide chains, which can be used to understand e.g. their superior mechanical properties.

Methods

The strong interaction between an electron probe and matter enables the acquisition of scattering data from nanometer-sized volumes even from weakly scattering elements. Electron diffraction has proven to be an invaluable tool for the structural examination of a diverse range of nanomaterials. Scanning electron diffraction (SED) offers detailed maps that reveal the crystalline ordering at the nanometer scale, shedding light on the arrangement of polysaccharide chains within individual nanofibers and also their hierarchical assemblies in composite materials.

In this study, we are using a quasi-parallel electron beam, with a convergence angle of 0.1 mrad. The beam is scanned across the specimen to obtain a map containing information about the molecular scale ordering of the biomaterial. The high speed and sensitivity of hybrid detectors enable the acquisition of electron diffraction data from single cellulose nanofibers.

Results

Cellulose nanofibers (CNFs) can be extracted from various origins and stand out as a promising, sustainable building block with remarkable mechanical properties. Using SED data, the crystalline nanostructure within individual CNFs can be analyzed, offering insights into how the crystalline ordering persists. Data was obtained from twisted sections of the nanofibers and reveals that despite the strain this twisting introduces the crystalline structure remains intact.[1] Furthermore, SED data can be employed to investigate the hierarchical organization of cellulose fibrils within the plant cell walls as well as hybrid materials based on wood. One prominent example of this is a composite material made from delignified and polymer-impregnated wood, the so-called transparent wood. SED data obtained from this material revealed the organization of cellulose fibrils into hierarchical helical structures across the various cell wall layers.[2] In most of the cell wall the cellulose fibers were organized along the extended dimension of the cells and towards the outermost part of the wall the fiber orientation gradually changed to a tangential orientation.

Conclusion

Using scanning electron diffraction we can for the first time reveal the molecular ordering of cellulose chains in twisting cellulose nanofibers as well as shed light on the mesoscale hierarchical ordering of cellulose fibers in hybrid materials and cell structures with nanometer resolution.

Keywords:

Scanning electron diffraction, biopolymer, cellulose,

Reference:

1. T. Willhammar, K. Daicho, D. N Johnstone, K. Kobayashi, Y. Liu, P. A. Midgley, L. Bergström, T. Saito ACS Nano 2021, doi: 10.1021/acsnano.0c08295
2. M. Nero, H. Ali, Y. Li, and T. Willhammar, "The Nanoscale Ordering of Cellulose in a Hierarchically Structured Hybrid Material Revealed Using Scanning Electron Diffraction" Small Methods, Dec. 2023, doi: 10.1002/smt.202301304.

526

Cryogenic electron microscopy for native state analysis of soft- and nano-materials

Dario Luis Fernandez Ainaga¹, Teresa Roncal-Herrero¹, Martha Ilett¹, Stuart Micklethwaite¹, Zabeada Aslam¹, Eleena Naveed¹, James Hitchcock¹, Cheng Cheng¹, Benjamin Lobel¹, Olivier Cayre¹, Dr Nicole Hondow¹

¹University of Leeds, Leeds, UK

PS-07 (2), Plenary, August 30, 2024, 10:30 - 12:30

Background

Nanomaterials can potentially be used in a range of areas, including in consumer goods through to medical applications. In many areas, the nanomaterials are used while dispersed in a liquid, or contain hard-soft interfaces, which, while increasing their applicability to their end-use, can complicate characterisation and determination of structure-property relationships.

Electron microscopy, while ideally suited to the nanoscale imaging and analysis of these materials, can encounter limitations due to the vacuum requirements, which exclude many in situ or native state studies. In addition, necessary sample preparation can often lead to artefacts. A viable alternative is electron microscopy conducted on frozen hydrated samples, where the nanomaterials are 'captured' in the native state and any electron beam induced damage products are immobilised. This work aims to develop representative native state analysis of dispersed nanoparticles in soft materials using cryogenic electron microscopy approaches, with application shown here to a commercial sunblock sample containing metal oxide nanoparticles and Pickering emulsions (water-oil mixtures) designed to contain an active ingredient.

Methods

Results from two soft materials containing dispersed nanoparticles will be detailed. The first sample is a Pickering emulsion, comprised of oil in water droplets stabilised by ~5 nm platinum nanoparticles. The approaches are further developed by examining a commercial product, a sunscreen containing active ingredients of 4.5% of TiO₂ and 6.5% of ZnO nanoparticles. All samples were prepared for cryo-TEM using an FEI Mark IV Vitrobot®. A 3.5 µl drop of suspension was loaded onto a lacey carbon-coated copper TEM grid (EM resolutions) before being blotted and then rapidly plunge frozen in liquid ethane. Transfer into the microscope was done using a Gatan-914 cryo TEM holder, and the temperature was maintained below -165 °C during analysis. Comparison was made to a static liquid cell (LC) commercially sold as a K-kit and supplied by Bio-Matek. S/TEM analysis was carried out using an FEI Titan3 Themis G2 equipped with a monochromator operating at 300 kV and fitted with 4 EDX silicon drift detectors and a Gatan One-View CMOS camera. The probe current was kept below 100 pA for all cryo and LC experiments. Samples were prepared for cryo-SEM using a Quorum Technologies PP3010 Cryo-SEM preparation system and examined in an FEI Helios G4 CX Dual beam FIB-SEM with a beam voltage of 1–10 kV and beam current 100 pA, while elemental mapping via an Oxford instruments EDX spectroscopy system was conducted at 15 kV.

Results

We have previously shown the advantage of cryogenic-EM approaches to the analysis of dispersed nanoparticles, including those in complex biological cell culture [1,2]. In this work we will show the advantages of using a cryogenic approach for more complex soft materials systems incorporating nanoparticles, with extension to the use of cryo-STEM-tomography and cryo-FIB-SEM.

Cryo preparation, transfer and analysis is essential for Pickering emulsions as the integrity of the sample is maintained as drying and the microscope vacuum results in bursting of the droplets. Undertaking higher magnification imaging with careful consideration of total electron fluence it is

possible to examine the distribution of the nanoparticles using cryo-STEM [3], and we will show that utilising cryo-HAADF STEM over a $\pm 60^\circ$ tilt range permits 3D visualisation of the sample structure. This results in the confirmation of both the position of the stabilising nanoparticles and the overall droplet shape in 3D space. Using a combination of cryo-EDX and -EELS the elements in both the nanoparticles and oil droplets are confirmed.

Cryo-STEM and associated spectroscopies are also used to analyse the commercial sunscreen, with comparison to alternative in situ electron microscopy techniques – static liquid cell STEM and cryo-SEM [4]. While cryo-STEM does allow for higher resolution analysis, in this case both the concentration of dispersed particles and viscosity of the product causes complications with sample preparation. In analysis of a diluted product, both nanoparticle types are identified, something which was not possible in the static liquid cell due to electron beam artefacts causing dissolution of one nanoparticle type. Cryo-SEM was used to analyse the pure product without dilution but biased the characterisation to the larger fraction of nanoparticles and agglomerates.

Conclusions

Cryo electron microscopy offers route to the representative native state analysis of dispersed nanoparticles in soft materials. Complex systems, such as the soft hybrid inorganic-organic Pickering emulsions can be analysed by a combination of STEM-analytical techniques to provide nanoscale 3D information. Commercial products, with numerous components and required to be used at a set concentration can be more complicated, however with a combination of different in situ EM techniques an accurate, native state characterisation can be achieved.

Keywords:

cryo; STEM; cryo-SEM; nanomaterials

Reference:

- [1] M Ilett, O Matar, F Bamiduro, S Sanchez-Segado, R Brydson, A Brown and N Hondow (2020) *Scientific Reports* 10, 5278.
- [2] M Ilett, R Brydson, A Brown and N Hondow (2019) *Micron* 120, 35.
- [3] J Hitchcock, AL White, N Hondow, TA Hughes, H Dupont, S Biggs and OJ Cayre (2020) *J Colloid Interface Sci* 567, 171.
- [4] M Ilett, E Naveed, T Roncal-Herrero, Z. Aslam, S. Micklethwaite and N Hondow (2023) *J Nanopart Res* 25, 122.

693

Investigating the chemical oxidative polymerization of 1,8 - dihydroxynaphthalene using a correlative in-situ approach

Dr Nivedita Sudheer^{1,2}, Kevin Ziegler³, Emmanuel Maisonhaute⁴, Vincent Ball³, Cédric Boissière⁵, Tom Ferte², Dris Ihiawakrim², Clement Sanchez^{1,5}, Ovidiu Ersen²

¹Collège de France, Paris, France, ²Institut de physique et chimie des Matériaux de Strasbourg (IPCMS), Strasbourg, France, ³Institut national de la santé et de la recherche médicale (INSERM), Strasbourg, France, ⁴Laboratoire Interfaces et Systèmes Electrochimiques (LISE), Paris, France,

⁵Laboratoire de Chimie de la Matière Condensée de Paris (LCMCP), Paris, France

PS-07 (2), Plenary, august 30, 2024, 10:30 - 12:30

Melanins, ubiquitous natural pigments found across various life forms, possess diverse biological functions such as camouflage and radioprotection. Notably, allomelanins derived from 1,8 - dihydroxynaphthalene (1,8-DHN) in Ascomycetes demonstrate robustness, offering protection against hostile environments. Despite their structural complexity and insolubility in solvents, allomelanins exhibit unique physical and chemical properties, including broad-band visible-light absorption, free radical characteristics, water-dependent conductivity, and redox behavior, albeit their exact structure remains incompletely defined[1], [2]. Thin films derived using chemical oxidative polymerization from physiologically active chemicals such as polyphenols have been studied to exhibit remarkable versatility across diverse substrates[3], [4], [5]. This study presents an in-depth investigation utilizing in-situ correlative microscopy and surface electrochemical methodologies to scrutinize thin films formed via the oxidative polymerization of 1,8-DHN molecules in aqueous electrolytes.

The study showcases the electrodeposition of 1,8 DHN onto gold electrodes and glassy carbon electrodes through cyclic voltammetry under in-situ liquid TEM using a miniaturized electrochemical cell. The resulting films demonstrate adjustable thickness and swelling properties, modulated by varying the potential sweep rate (20mV/s, 200mV/s and 1000mV/s). Analysis of the films' surface characteristics is conducted through Raman-coupled electrochemical spectroscopy and in-situ ellipsometry, complemented by cyclic voltammetry to explore their electrochemical behavior. Additionally, employing in-situ TEM provides insights at the nanoscale, in direct space into the electrochemical mechanisms occurring during the film formation.

Through the application of in-situ liquid TEM using an electrochemical cell, the real-time mechanism of thin film formation during electrodeposition has been elucidated, marking a significant advancement in the field. A proposed mechanism for the oxidative polymerization of 1,8 DHN is supported by Raman-coupled electrochemical spectroscopy, indicating dimer formation during the initial stages. Additionally, concurrent analysis with in-situ ellipsometry has allowed for the simultaneous investigation of the relationship between film thickness, scan rates, and optical properties, while quasi-in-situ impedance spectroscopy has provided insights into the electrical and conducting properties of these polymers in relation to the sweep rates. Notably, these films exhibit inherent antioxidant properties with antioxidant components distributed throughout the films' structure within a restricted energy range of -1 V to +1 V versus Ag/AgCl.

From a material point of view, this correlative study which includes in-situ liquid TEM analyses highlights the considerable potential of employing mild electrochemical conditions to fabricate electropolymerized thin films via the Chimie-Douce mechanism utilizing fundamental organic constituents. Moreover, combining several in-situ techniques including electrochemical TEM, Raman coupled electrochemical spectroscopy, and ellipsometry, we bring new insights into chemical

oxidative polymerization at different scales and more generally a structural evolution during electrochemical phenomena. Given their insolubility in commonly used solvents and favorable mechanical properties, these films hold promise as protective coatings. Moreover, their electroactive and antioxidant properties render them highly suitable for a wide range of applications, including environmental remediation, biomedicine, and catalysis.

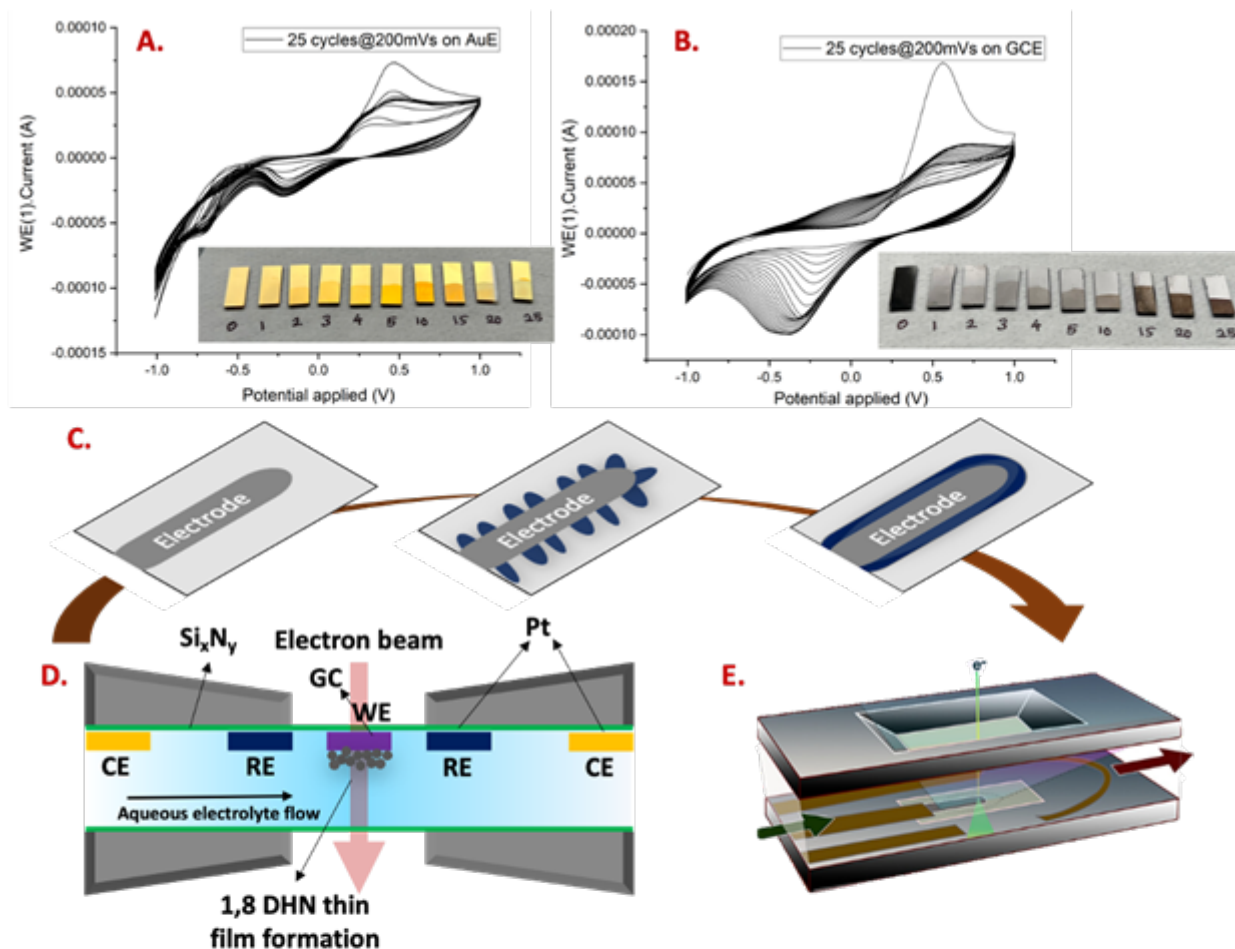


Figure 1. The figure illustrates the chemical oxidative polymerization and deposition of 1,8 DHN on the WE (Au and glassy carbon) which will be characterized using complimentary cyclic voltammetry techniques. (A) Cyclic voltammogram of 1,8 DHN at 25 cycles in 200mV/s on Au electrodes and the gradual formation of thin films with the number of cycles observed in the picture, (B) Cyclic voltammogram of 1,8 DHN at 25 cycles in 200mV/s on glassy carbon electrodes and the gradual formation of thin films with the number of cycles observed in the picture, (C) Illustration of formation of thin films on the working electrodes, (D) Transversal schematic view of the assembled cell. WE, CE and RE are the working, counter and pseudo-reference electrodes, respectively. GC is the glassy carbon current collector in the WE. (E) Side schematic view of an assembled cell.

Keywords:

In-situ-liquid TEM, Raman-coupled electrochemical spectroscopy

Reference:

1. Cecchini, M. M., Reale, S., Manini, P., d'Ischia, M. & De Angelis, F. Modeling Fungal Melanin Buildup: Biomimetic Polymerization of 1,8-Dihydroxynaphthalene Mapped by Mass Spectrometry. *Chemistry – A European Journal* 23, 8092–8098 (2017).
2. Lino, V. & Manini, P. Dihydroxynaphthalene-Based Allomelanins: A Source of Inspiration for Innovative Technological Materials. *ACS Omega* 7, 15308–15314 (2022).
3. Myers, R. E. Chemical oxidative polymerization as a synthetic route to electrically conducting polypyrroles. *J Electron Mater* 15, 61–69 (1986).
4. Gospodinova, N. & Terlemezyan, L. Conducting polymers prepared by oxidative polymerization: polyaniline. *Prog Polym Sci* 23, 1443–1484 (1998).

5. Higashimura, H. & Kobayashi, S. Oxidative Polymerization. in Encyclopedia of Polymer Science and Technology 1–37 (Wiley, 2016). doi:10.1002/0471440264.pst226.pub2.

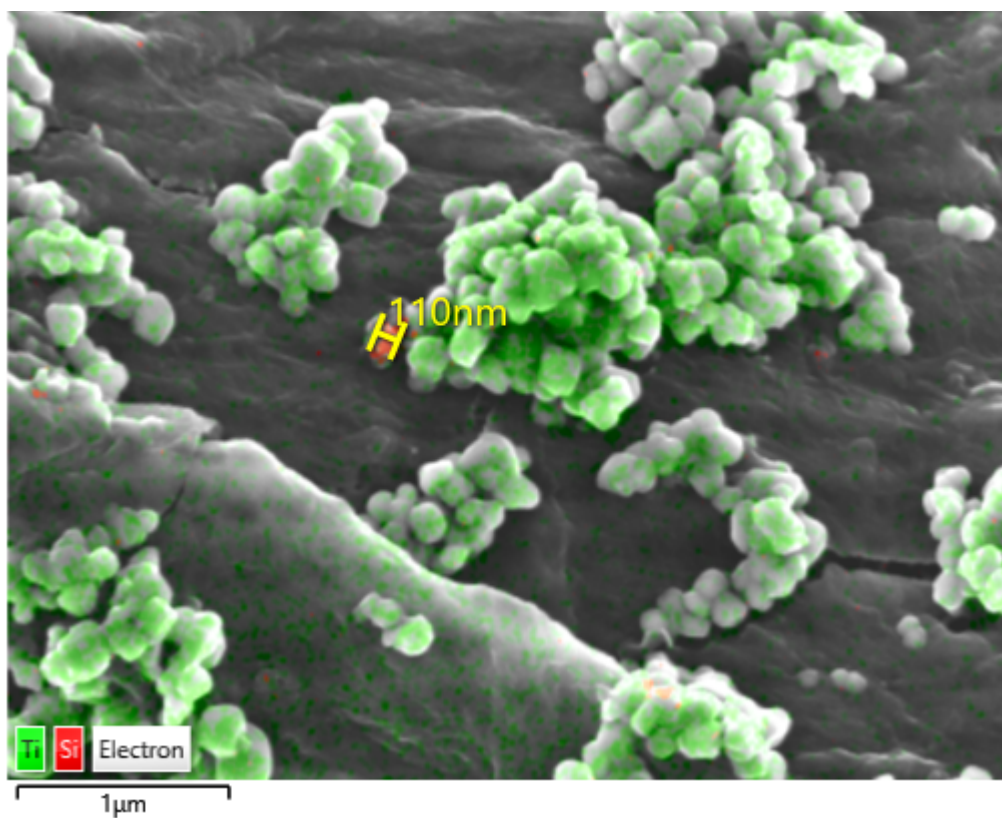
Examination of the Thermal and Morphological properties of Spartium Junceum Fibers for Flame Retardant Purposes

Zorana Kovacevic¹, Mrs. Lucia Spasevski², Prof.Dr. SANDRA BISCHOF¹

¹University of Zagreb Faculty of Textile Technology, Zagreb, Croatia, ²Oxford Instruments NanoAnalysis, High Wycombe, United Kingdom

Poster Group 2

Fibers isolated from the *Spartium junceum* L. – plant which is indigenous to the Mediterranean area (S JL), belongs to a group of the plant bast fibers. Taking into the account previous research, it is proven to be an excellent fibrous raw material which, among others things, can play a role as a reinforcement in the production of fiber-reinforced composite materials. Nowadays, due to the increasing environmental awareness and the need to reduce negative impact of production by-products on climate, there is an effort to develop new materials from sustainable sources. Such materials can be functionalized through targeted ecologically acceptable surface modifications. The fire risk control is a very important concept in all branches of industry, especially in the automotive where the property of reduced flammability of the materials is very desirable. In order to meet such demands bast cellulosic fibers that are easily flammable need to be modified. In this research, S JL fibers were specifically treated with silicon dioxide, aluminum oxide and titanium dioxide nanoparticles that were fixed on the fiber surface using microwave irradiation or contact heat transfer (hot press). SiO₂ (SiNPs) and Al₂O₃ (AlNPs) nanoparticles were produced by laser ablation in liquid using a high power laser which ablates the metal plates without surfactant or aggressive chemicals addition. S JL fibers were treated with 0.025% aqueous solution of SiO₂ and Al₂O₃ nanoparticles and 2% of TiO₂ (TiNPs) nanoparticles, respectively by using ultrasound technique. Examination of the thermal and morphological properties of functionalized fibers were performed using thermogravimetric (TGA), microscale combustion calorimetry (MCC), scanning electron microscopy (SEM) & energy dispersive spectroscopy-EDS (backscatter electron and X-ray technique (BEX), X-MaxN 150 detector, ULTIM Max 100 detector and Ultim Extreme detector). For the samples fixed with the contact heat transfer heat release and thermal decomposition results are exhibit same properties as untreated sample and were therefore excluded from the further analysis. The best results were achieved by treatment with Al₂O₃ and TiO₂ nanoparticles which were fixed to fiber surface with microwave irradiation. According to the MCC analysis Heat release capacity (HRC) and Peak heat release rate (PHRR) measure the amount of the heat which is generated throughout the combustion process and the maximum rate of the heat release, respectively. In these samples, a significant reduction of the heat release rate (HRR) peak is visible (From 157 W/g for untreated to 137 W/g for AlNPs treated fiber). AlNPs treated sample show a later start of the decomposition in comparison to the untreated sample at approx. 386 °C. TGA analysis shows a residual char yield increase in all treated samples confirming their better flame retardancy in comparison to the untreated sample. Untreated fiber starts to decompose at approx. 345 °C and ends at approx. 686 °C, while thermal decomposition for fiber treated with AlNPs ends at approx. 711 °C. Considering the very small amount of deposited SiO₂ and Al₂O₃ nanoparticles and the sheer size of them on the surface of the fiber, several different mapping approaches for chemical elements determination were compared. BEX technique was proven to give best results for quick inspection of large surface area due to combination of BSE imaging and high throughput EDS sensors. While for more detailed inspection, to confirm the presence of a small concentration of nanoparticles on S JL fiber surface Ultim Extreme was proven to be the best solution that can provide enough X-ray signal even at low voltage (3kV) and low beam current (700pA) conditions necessary to image nanoparticles.



Keywords:

bast fibers, SEM, EDS, BEX

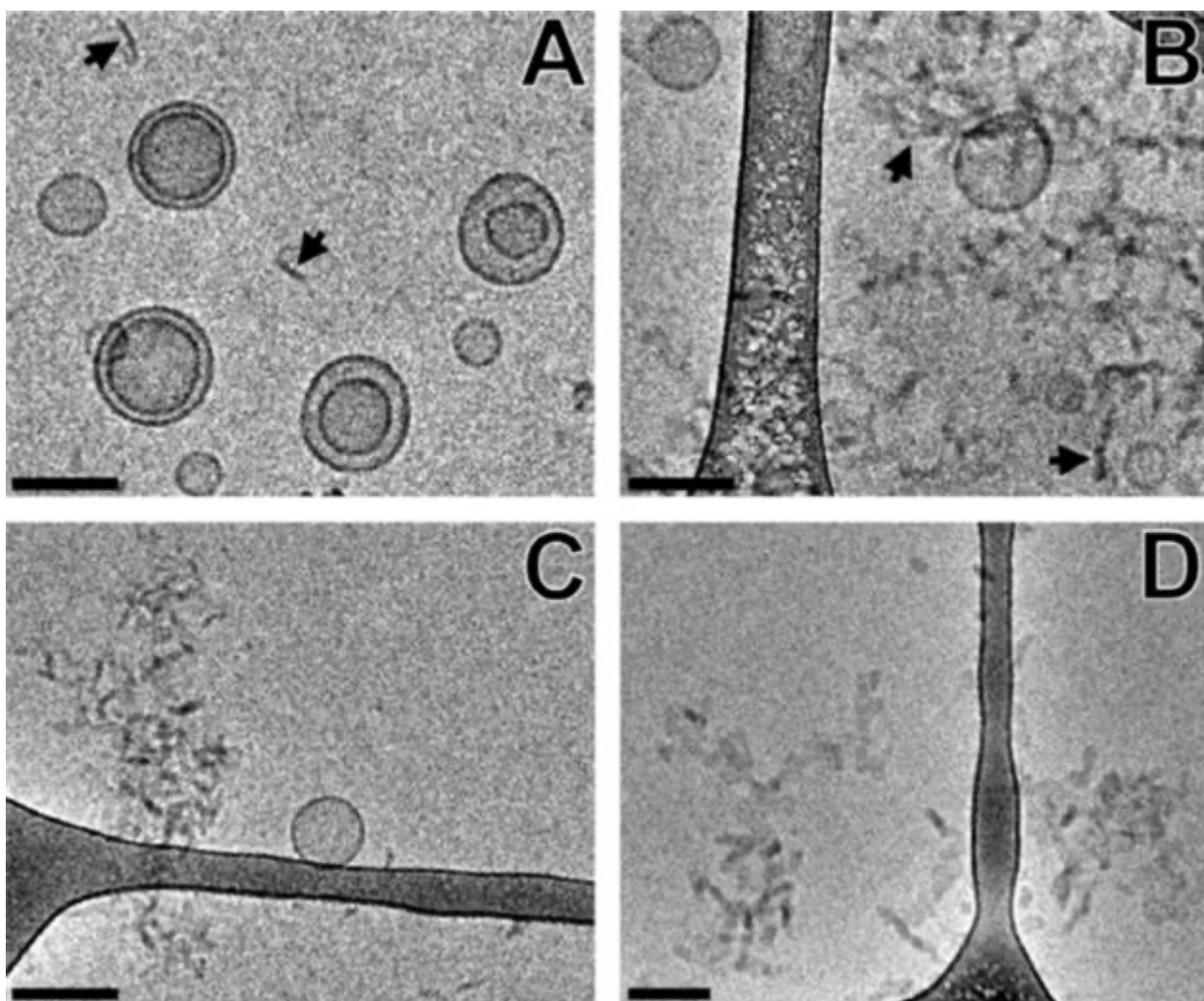
TRIBLOCK POLY(2-OXAZOLINE)S WITH A FLUORINATED BLOCK AS A NEW PLATFORM FOR ADVANCED SELF-ASSEMBLY: CRYO-TEM STUDY

Sergey Filippov¹, Dr. Leonid Kaberov², Dr. Lubomir Kovacic³, Prof. Richard Hoogenboom⁴

¹DWI Institute of Interactive Materials, Aachen, Germany, ²Friedrich Schiller University, Jena, Germany, ³C-CINA, Biozentrum, University of Basel, Basel, Switzerland, ⁴Ghent University, Ghent, Belgium

Poster Group 2

The synthesis of defined triphilic terpolymers with hydrophilic, lyophilic, and fluorophilic blocks is an important challenge as a basis for the development of multicompartiment self-assembled structures with potential for, e.g., cascade catalysis and multidrug loading. A series of fluorinated 2-substituted-2-oxazoline copolymers with hydrophilic 2-methyl-2-oxazoline, hydrophobic 2-octyl-2-oxazoline, and fluorophilic blocks were synthesized in our group previously [1-5]. The presence of the blocks with the different nature in one copolymer structure facilitated self-assembly of the copolymers in water as observed by dynamic light scattering, and cryo-transmission electron microscopy. The nanoparticle morphology is strongly influenced by the order and length of each block and the nature of solvent, leading to nanoparticles with tuning structure as confirmed by Cryo-TEM. For the polymer that has no fluorinated tail formed primarily multi-layered vesicles (Figure 1A), which is in agreement with the DLS result. In contrast, the cryo-TEM analysis of the polymer solution with shortest fluorinated block showed a mixture of aggregating rod-like micelles and little-populated single-layered vesicles (Figure 1B). However, the extension of the fluoroalkyl chain length further decreased the relative content of the vesicles (Figure 1C). This trend is continued for copolymer with the longest fluorinated alkyl chain, which only showed isolated rod-like micelles with a small fraction of agglomerates composed of rod-like micelles, while vesicles were no longer observed (Figure 1D). Figure 1. Cryo-TEM images of the investigated polymers. (A) The non-fluorinated diblock copolymer formed single- and multi-layered vesicles, together with short rod-like micelles. (B) The C8F17 and C) C10F21 copolymers formed single-layered vesicles and aggregates of rod-like micelles. (D) The C12F25 copolymer assembled into rod-like micelles only. Scale bars: 100 nm. The reported poly(2-oxazoline) block copolymers with high fluorine content have high potential for future development of MRI contrast agents.



Keywords:

polymers, poly-2-oxazolines, self-assembly, micelles, vesicles

Reference:

- [1] Leonid Kabarov, et.al. *European Polymer Journal*, 2017, 88, 645-655.
- [2] Anna Riabtseva, et.al., *European Polymer Journal*, 2018, 99, 518-527.
- [3] Leonid Kabarov, et.al., *ACS Macro Lett.* 2018, 7, 7–10.
- [4] Leonid Kabarov, et.al., *Macromolecules*, 2018, 51 (15), 6047-6056.
- [5] Leonid Kabarov, et.al., *Biomacromolecules*, 2021, 22(7), 2963-2975.

Optimizing micrograph contrast in multicomponent systems at low-voltage scanning electron microscopy

Asia Matatyaho Ya'akobi¹, Irina Davidovich¹, Yeshayahu Talmon¹

¹The Department of Chemical Engineering and The Russell Berrie Nanotechnology Institute (RBNI), Haifa, Israel

Poster Group 2

Background incl. aims:

Scanning electron microscopy (SEM) is one of the most widely used electron microscopy techniques in science and engineering. Although the SEM was originally intended for operation at low beam acceleration voltages (BAV), it was only possible to operate at low beam energies decades after the first commercial SEM was available. Hence, most of the pioneering studies of electron-specimen interaction physics have been conducted at BAVs above 5 kV. In recent years, the reliable and easy-to-operate field emission guns (FEGs), and the improved optics, vacuum, and detectors in modern SEMs, have led to the widespread use of low-voltage SEM. However, studies in the low BAV range remain limited, and there is a lack of awareness of their importance. The purpose of this study is to investigate the effects of SEM operational parameters and specimen properties on micrograph contrast at BAVs below 2 kV.

Methods:

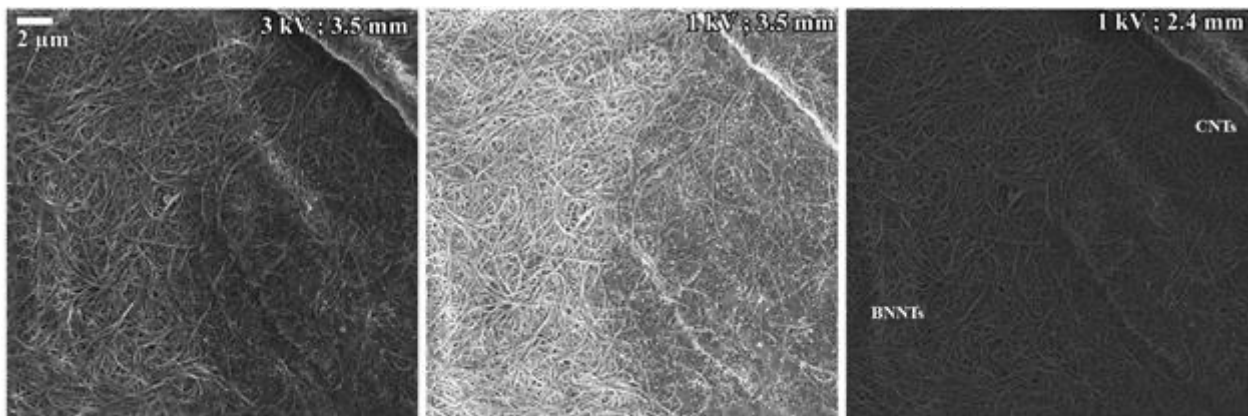
The modern SEMs, equipped with the in-the-column ("InLens" in the Zeiss lingo) secondary electron detector for high-resolution imaging, are flexible instruments allowing operation over a wide range of parameters. Two of the fundamental SEM operational parameters are the BAV and the working distance (WD). Here, we investigate systematically the effect of the BAV and the WD on the InLens micrograph contrast. We image a variety of specimens, consisting of conductive (carbon nanotubes) or insulating (boron nitride nanotubes) materials, or their combination, on conductive (silicon wafer) and insulating (glass slide) substrates. To include all combinations, we imaged 6 specimen types, each specimen was imaged at 3 different BAVs, where at each BAV the micrograph was acquired at 3 different WDs.

Results:

Our results show that the InLens micrograph contrast is directly affected by the BAV and the WD, and by the specimen electrical conductivity properties. We analyze the contrast changes and explain them through the changes in the secondary electron signal at different conditions. We demonstrate that choosing adequate SEM operational parameters is essential for obtaining an optimal micrograph contrast, and thus for obtaining complete information of the specimen. Moreover, in the case of insulating specimens, we demonstrate the possibility of avoiding specimen charging without using conductive coating.

Conclusions:

For proper selection of the SEM operational parameters, one should understand how micrograph contrast changes with BAV and WD, and be able to adjust them according to specimen properties. This way, an optimal micrograph with sufficient contrast but without charging artifacts can be obtained. As our study includes a variety of systems combining conductive and insulating components, its conclusions can be easily adopted for a wide range of systems and studies.



SEM InLens micrographs of a dense region in a mixed specimen of CNTs and BNNTs deposited on a glass slide. The same area of the specimen imaged at different imaging parameters. With proper selection of the imaging parameters, contrast between the two types of nanotubes can be obtained.

Keywords:

Low-voltage SEM, micrograph contrast

A Secondary Electron Hyperspectral Imaging characterisation of mechanochemically functionalised carbon black materials

James Nohl^{1,2}, Nicholas Farr¹, Maria Rosaria Acocella³, Serena Cussen⁴, Cornelia Rodenburg¹

¹Department of Materials Science and Engineering, The University of Sheffield, Mappin Street, Sheffield, UK, ²The Faraday Institution, Quad One, Becquerel Avenue, Harwell Campus, Didcot, UK,

³Department of Chemistry and Biology "A. Zambelli", University of Salerno, Via Giovanni Paolo II, 132- 84084 Fisciano, Italy, ⁴School of Chemistry, University College Dublin, Belfield, Dublin 4, Ireland

Poster Group 2

Background

Carbon blacks find applications in composite materials for energy generation and storage, structural materials, as well as catalysis and as precursor materials. In nanocomposite applications of carbon black, the surface functionalisation of the carbon black is important in determining the structure of the composite and the function of the material [1]. Powders in this form are often characterised as a bulk material, however it is important to understand the local surface chemistry and distribution of chemistries between particles, particularly when the surface of the powder is engineered to achieve certain properties.

Such is the case with carbon black subject to surface oxidation processes. In this case, a one-step ball milling process was used to vary the particle morphology and surface oxidation [2]. X-ray photoelectron spectroscopy (XPS) can tell average oxidation. Transmission electron microscopy (TEM) can tell particle size and surface chemistry – but not for in-situ satellite particles. Therefore, a study which includes local information about particle morphology and functionalisation with process time, may offer insight into the dynamics of the process which includes fracturing, agglomeration, exfoliation and oxidation.

Secondary electron hyperspectral imaging (SEHI) proved to be a valuable technique for characterisation of polymers functionalised by plasma surface treatment [3]. Here we show the technique is applicable to a nano materials characterisation challenge to image the morphology and local surface chemistry of satellite particles in-situ produced during milling on bulk carbon black particles.

Methods

The carbon blacks characterised by SEHI were as-received carbon black and carbon black ball milled without solvent at room temperature for a total of 0h, 1h, 5h, 9h and 11h. Average spectra from 20 μm horizontal field width images were produced for the as-received carbon black and each ball milling process time. A functionalised carbon black model was fitted to spectra to obtain component peak heights using the `lmfit` python module (Figure 1a). Ratios of peak heights for CH (hydrogenated amorphous carbon) and OH functionalised carbon to sp^2 -hybridised graphitic carbon were calculated (Figure 1b). The energy ranges 2.2-2.8 eV, 3.0-3.6 eV, 4.2-4.9 eV and 5.4-6.0 eV were used to create colour maps related to sp^2 , CH, OH and $\text{CO}+\text{sp}^3$ surface functionalities respectively (Figure 1c). These component images were assigned to channels with hue values equidistantly spaced in the HSV colour space (Figure 1d). The composite map is a sum of these component images (Figure 1e).

Results

The CH: sp^2 ratio decreases from 1.05 to a minimum of 0.5 at 5h milling time, then increases to 1.4 at 11h. The OH: sp^2 ratio decreases from 1.3 to a minimum of 0.8 at 5h milling time then increases to a maximum ratio obtained by processing of 1.3 at 9h. Further milling to 11h decreases the OH: sp^2 ratio to 1.1 (Figure 1b). The results indicate that the sp^2 surface content is maximum at 5h. Further milling

up to 9h oxidises the surface but more milling post 9h produces more amorphous hydrogenated carbon surfaces.

At 5h, the composite colour map indicates a nanoscale 'satellite' particle morphology (see Figure 1d inset for a line profile indicating the particle size) with strongest emissions in the OH component range.

Conclusions

SEHI added to the understanding of the carbon black material by analysing the local chemistry of 'satellite' nano particles which were more oxidised versus the bulk carbon black particle. This is not clear from spatially averaged XPS analyses of the powder.

Meanwhile, a spatially averaged SEHI analysis identified components for carbons and surface carbon compounds. A qualitative comparison of the CH and OH to sp^2 ratios versus ball milling time in oxidative conditions showed a maximum of sp^2 surface chemistry by 5h before this was oxidised to the highest OH: sp^2 ratio at 9h and the highest CH: sp^2 at 11h.

Local characterisation enhances understanding of how the processing influences surface chemistry and morphology resulting from process time.

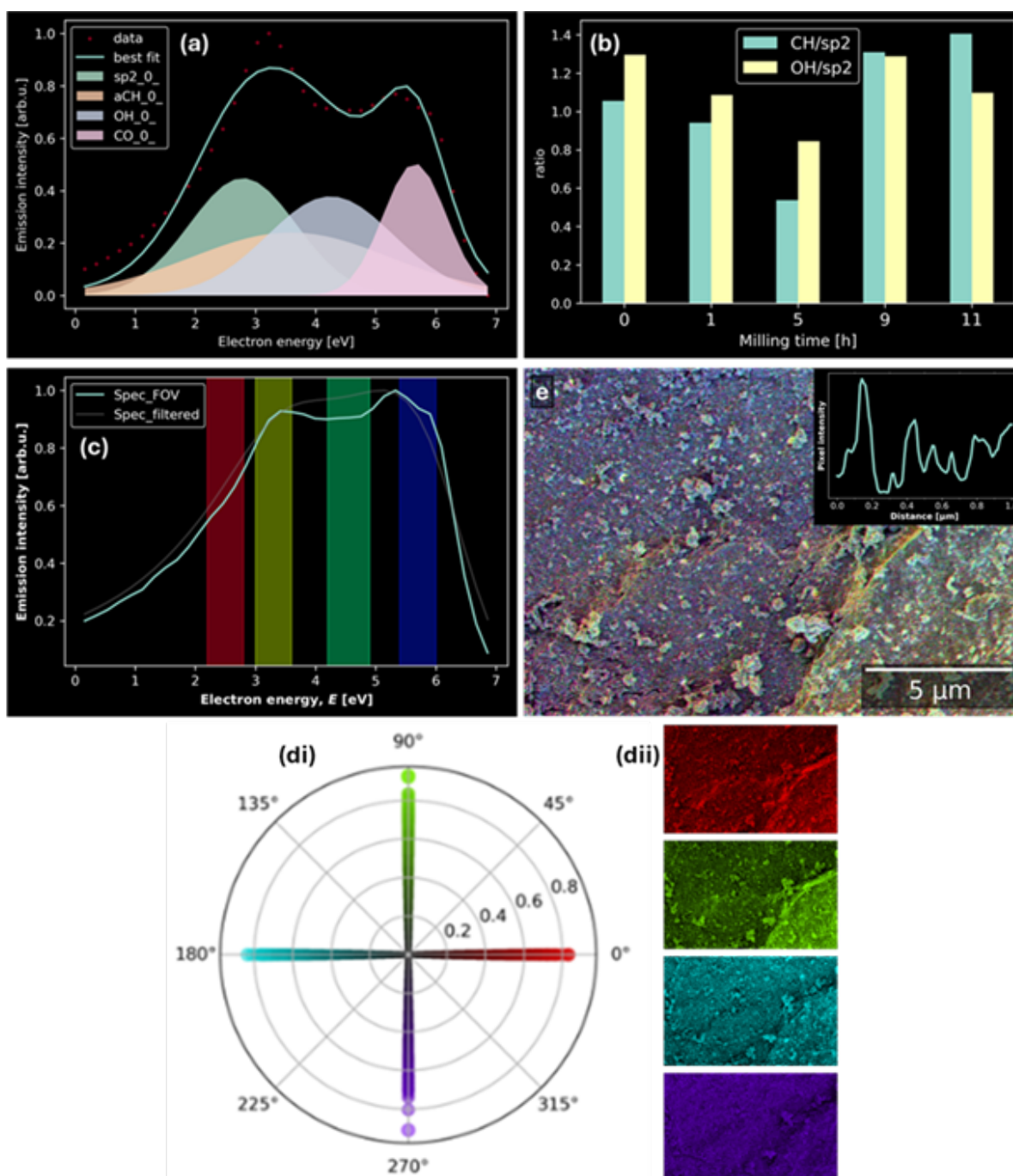


Figure 1 – (a) Component fit to average SE spectra for material produced by 5h ball milling. (b) CH:sp² and OH:sp² ratio plots for each ball milling time. (c) energy ranges assigned to spaced colour hue channels (fi) to make component images (fii) summed to make the colour image in (e). (e – inset) line profile showing nanoscale satellite particle morphologies.

Keywords:

Carbon black; SEHI; SEM; oxidation

Reference:

- [1] C. Shepherd et al., *Langmuir* 2016 32 (31), 7917-7928, DOI: 10.1021/acs.langmuir.6b02013
- [2] Aida Kiani, M. Rosaria Acocella, et al., *ACS Sustainable Chemistry & Engineering* 2022 10 (48), 16019-16026, DOI: 10.1021/acssuschemeng.2c05638
- [3] N. Farr et al., *Adv. Sci.* 2021, 8, 2003762, DOI: 10.1002/adv.202003762

153

Probing chemical pathways in polymer membranes despite electron beam damage

Dr Catriona M. McGilvery¹, Dr Patricia Abellan², Prof Quentin M. Ramasse³, Prof Alexandra E. Porter¹

¹Imperial College London, London, UK, ²CNRS-Nantes University, Nantes, France, ³SuperSTEM Laboratory, Daresbury, UK

Poster Group 2

Reverse Osmosis (RO) membranes are used for seawater desalination in the oil and gas industry. These membranes are made of a polyamide (PA) 'active' layer, around 100-500 nm thick, a polysulfone (PSf) support and a polyester backing layer. The PA layer is thought to control ion flow through the membrane yet very little is understood about how that is achieved at the nanoscale. A number of techniques have been used to try to characterise the PA layer but none of them have the spatial and energy distribution necessary for nanoscale chemical mapping. Here we test whether scanning transmission electron microscopy EELS (STEM-EELS) techniques can be used to map chemical functionality across flat RO membranes with nm-scale resolution. We argue that, despite the high electron flux required during acquisition, careful comparison to dose-managed control experiments on standards together with multivariate analysis post-processing techniques can be used to extract useful information about the distribution of functional chemistry from spectra acquired from damaged PA.

Practically, commercial RO membranes are very rough making them difficult to characterise. For this reason, in-house prepared 10 nm thick PA membranes prepared via an interfacial polymerisation technique, were used for this study. STEM EELS studies were carried out on a Nion UltraSTEM 100MC 'HERMES' monochromated transmission electron microscope at SuperSTEM (Daresbury, UK). The microscope was operated at 100 kV with a probe size of 0.9 Å and convergence and collection semi angles of 31 and 44 mrad respectively.

First, chemical maps of C, N and O K-edges, the main components of the membranes, were obtained. From the nitrogen signal the exact width of the membrane could be established as N is only present in the membrane itself. Control beam damage studies were carried out on large areas (800 nm x 800 nm) of plan-view samples so that the degree of damage on the C K-edge could be assessed. The parameters required to avoid detection of beam damage effects were impractical for obtaining chemical information with a pixel size of 2 nm. However, with higher electron fluences (e.g. 3-10 x 10⁷ e/Å² per probe size or 6-10 x 10³ e/Å² per pixel size), whilst damage occurred to the carbon bonds, the dominant features in the fine structure of the C K-edge were in fact still present and variations could be mapped across the PA membrane with a spatial sensitivity of 2 nm. Application of multivariate analysis to the raw high electron fluence data made it possible to assign peaks related to specific co-ordination environments by comparison with the control data fine structure.

This work shows that despite severe electron beam damage evident by the loss of fine structure of the C K-edge, information about functional chemistry within the PA can still be achieved. This suggests that spectra obtained where the electron flux has been high, may still be interpreted provided care is taken to assess the extent of possible beam damage and carry out control experiments. With continued advancement of technologies such as stable cold stages, high frame rate cameras and direct electron detection capabilities it should become easier to map functional chemistry across radiation sensitive soft materials with nm-scale high spatial and energy resolution.

Keywords:

polymers

EELS

beam-damage

chemical pathways

407

Towards advanced polymer membranes for hydrogen technologies through dose-optimised Focused Ion Beams

Dr Ofentse Makgae¹, Dr Martha Briceno de Gutierrez¹

¹Johnson Matthey Technology Centre, Reading, United Kingdom

Poster Group 2

Background & Aims

Understanding the properties of membranes applied in the CCMs of electrolyser and fuel cell technologies is crucial to advancing the commercialisation and deployment of these technologies to the market. The cross-sections of these membranes are typically studied using a Focused Ion Beam (FIB). A FIB is a technique in which accelerated (Ga) ions sputter material away upon interaction.¹ This technique is used mainly for electron-transparent transmission electron microscopy sample preparation, FIB tomography, or cross-sectional analysis of materials such as semiconductors, ceramics, metals, polymer thin films, and biological specimens. Unlike conductive materials such as ceramics and metals, polymer membranes are non-conductive and thus susceptible to beam-induced heating during ion beam milling.² Ion beam-induced heating in polymer membranes creates 'melt-like' artefacts that smear the pristine structural details of the membrane along the cross-section. In addition, it is also shown that accelerated Ga ions can result in the chemical alteration of the membrane's chemical structure, which affects the properties of the membrane.³ This ion-beam-induced damage is typically circumvented by dose-controlled milling or lowering the specimen temperature via cryogenics. Here, we aim to optimise the milling parameters for polymer membrane cross-section milling by determining the optimum current, accelerating voltage, and dwell time required to minimise beam-induced heating in polymer membranes.

Methods

Polymer membranes were mounted on SEM-FIB stubs and sputter-coated with a conductive layer of carbon. A series of cross-sections were milled using a Zeiss Crossbeam 550 dual-beam at a varying current, accelerating voltage, dwell time, and ion dose. The actual values will be presented with the results.

Results and conclusions

Preliminary results show that reducing the dwell time at low milling currents and high voltage reduces the beam-induced artefacts in the membrane cross-sections. The results of this study will help understand the pristine microstructure of polymer membranes in a standardised and reproducible routine cross-sectional analysis, and ultimately lead to the development of novel membranes for applications in hydrogen technologies.

Keywords:

FIB; Polymer membranes; ion damage

Reference:

1. L.A. Giannuzzi, F.A. Stevie., *Micron* 30 (1999) 197–204
2. S. Kim et al., *Ultramicroscopy* 111 (2011) 191–199
3. R.J. Bailey et al., *Micron* 50 (2013) 51–56

473

4D-STEM and EELS Analysis of Complex C-based Sensor Architectures

Mr Charles Otieno Ogolla¹, Mr Charles Otieno Ogolla¹, Mr Marco Hepp¹, Prof. Benjamin Butz¹, Tristan Zemke

¹University of Siegen, Siegen, Germany

Poster Group 2

Background

The transformation of precursors with high carbon content into open-porous carbon foams and coatings via thermal processes is gaining traction as a promising and eco-friendly method for a range of applications including catalysis, energy utilization, and sensing [1]. In this investigation, we employ a one-step laser patterning technique to locally pyrolyze doctor-bladed ink coatings on flexible PET substrates. This process yields highly porous and intricate CO₂ sensor architectures with a thickness of around 50 μm . The ink composition includes glucose as a pore-forming agent and adenine as a nitrogen source, contributing to the sensing capabilities. Laser treatment in an oxygen-rich environment results in flexible and highly porous sensor structures with distinct nitrogen and oxygen functionalities within different regions. The laser intensity varies with depth, leading to the creation of a well-defined highly porous graphitic surface layer (acting as the electric transducer layer) and a less porous nitrogen-rich lower sensor layer, interconnected by a thin transition zone [2].

Methods

To understand the formation of these structures and their relationship with functionality, we conducted a thorough TEM investigation on cross-sections (0.25 - 0.5 t/λ) of the entire device prepared by microtomic cross-sectioning.

Results & Conclusion

STEM-EELS elemental distribution maps reveal a clear distinction in chemical composition between the upper and lower layers of the sensor. Principal component analyses were utilized to unravel the complex sensor structures, comprising various crystalline and amorphous phases containing carbon and nitrogen. 4D-STEM analysis unveils the distribution of the crystalline graphitic phase and the alignment of graphite basal planes relative to the pore walls of the open-porous sensor. Understanding these parameters is crucial for deciphering the electrical performance of the sensor (refer to Figure 1) [3].

Acknowledgements: We acknowledge use of the DFG-funded Micro-and Nanoanalytics Facility (MNaF) at the University of Siegen (INST 221/131-1).

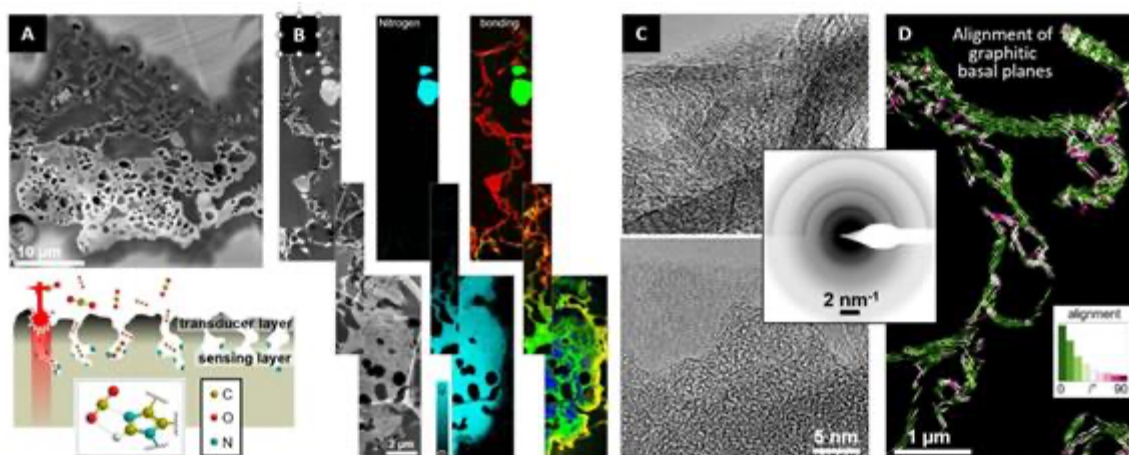


Figure 1. A) Top: A SEM micrograph displaying the sensor embedded in epoxy, Bottom: The attenuation of thermal laser intensity varying with depth. B) Left: A HAADF-STEM micrograph revealing distinct sensor layers, Middle: A STEM-EELS nitrogen distribution map, Right: PCA bond analysis. C) HRTEM images of the sensor from the transducer (top) and sensor (bottom) layers with corresponding SAED image of respective ROIs (inset). D) 4D-STEM analysis illustrating the misalignment angle between the normal of the graphitic carbon basal plane and the pore surface normal.

Keywords:

4D-STEM, open-porous carbon, laser pyrolysis

Reference:

- [1] M. Hepp, et al. *npj Flexible Electronics* 6, 1-9 (2022)
- [2] H. Wang, et al. *Advanced Functional Materials* 32, 2207406 (2022)
- [3] C. Ophus, et al. *Microscopy and Microanalysis* 28, 390-403 (2022)

490

Elucidating functionalities of N-doped carbonaceous materials by means of in-situ TEM

Dr Nadezda Tarakina¹, Dr. Diana Piankova¹, Dr. Hannes Zschiesche¹, Dr. Jing Hou¹, Prof. Dr. Markus Antonietti¹

¹Department of Colloid Chemistry, Max Planck Institute of Colloids and Interfaces, Potsdam, Germany
Poster Group 2

Background incl. aims

Nitrogen-doped carbonaceous materials gained broad interdisciplinary attention as low-cost, metal-free materials for photocatalysis, carbon capture, energy storage and water remediation. Their performance in real devices relies on the precise control of their nanostructure. Usually, nanostructural characterizations are done after completion of either the synthesis or the device operational cycle. Here we present two scientific questions related to functionalities of N-doped carbons, for which in-situ/in-operando TEM studies were crucial: (1) How N-doped carbons condensate from molecular precursors, and how can we thus guide their design as materials for CO₂-sorption¹ and (2) What is the nanoscale mechanism of Na storage in N-doped carbons when they are used as anodes in Na-batteries². The Methods and Results sections below are structured according to these two questions. Generalized conclusions on the application of the in-situ/in-operando methods to polymeric materials exemplified by N-doped carbons are given.

Methods

In this study we combined ex-situ high-resolution STEM, energy-filtered electron radial distribution function analysis, energy dispersive X-ray analysis and electron energy loss spectroscopy (at (1) different stages of condensation and (2) at different states of charge during electrochemical cycling) with in-situ STEM investigations: (1) in-situ heating was performed using a heating/biasing Protochips Fusion Select holder; (2) an in-operando Na half-battery was constructed using a Protochips Poseidon holder. 1 M solution of NaPF₆ in ethylene carbonate and diethyl carbonate was used as electrolyte.

Results

(1) By combining in situ condensation inside a STEM and ex situ analysis of the products of condensation at different temperatures and atmospheres, we were able to follow the structural, morphological, and chemical evolution of the uric acid and guanine precursors on the nanoscale upon heating and correlate it with the sorption properties of the obtained materials. We showed how one can control and tune the formation of pores in nitrogen-containing carbonaceous materials by varying pressures and reaction rates. We found that these two parameters change how the porosity of the surface develops, forming particles with mesopores (in vacuum) or microporous (in nitrogen) surfaces. Since this process co-occurs with cross-linking, the porous structure of the surface governs the subsequent release of volatiles and the development of the hierarchical pore structure. These findings allow us to synthesize N-doped carbons with a 2-times higher CO₂ uptake, keeping the same selectivity.

(2) N-doped porous hollow carbon spheres (N-PHCSs), which due to their size and shape, serve as an ideal model system to investigate Na-storage at the nanoscale, have been synthesized. By combining the ex-situ characterization at different states of charge with in-operando TEM experiments we found that at the beginning of sodiation a solvated ionic layer forms on the surface of N-PHCSs, followed by irreversible shell expansion due to the solid electrolyte interface formation and subsequent storage of Na(0) within the porous carbon shell. We showed that binding between Na(0) and C creates a Schottky junction making Na deposition inside the spheres more energetically favorable at low current densities. During sodiation, the solid electrolyte interface fills the gap

between N-PHCSs, binding spheres together and facilitating the Na ions' transport in the direction of the current collector and subsequent plating underneath the electrode. The N-PHCSs layer acts as a protective layer between the electrolyte and the current collector, suppressing possible growth of dendrites at the anode.

Conclusion

In situ/in-operando characterization, setups have been successfully applied to the characterization of N-doped carbonaceous materials. However, special attention is required for separating the electron-beam-induced effects and the processes we are interested in. The synergetic combination between ex-situ and in-situ experiments is crucial for obtaining realistic models of the studied processes.

We gratefully acknowledge financial support by the Max Planck Society. We are grateful to Dr. J. Kossmann, Dr. M. Odziomek and Prof. N. Lopez-Salas for help with synthesis, CO₂ sorption characterization and valuable discussions.

Keywords:

N-doped carbons, in-situ microscopy, batteries

Reference:

- [1] D. Piankova, J. Kossmann, H. Zschiesche, M. Antonietti, N. López-Salas, N. Tarakina, J. Mater. Chem. A, 2022, 10, 25220-229;
- [2] J. Hou, Z. Song, M. Odziomek, N. Tarakina, Small, 2023, 2301415.

576

Cryogenic large volume 3D and TEM sample preparation with multiple ion species plasma FIB

Dr. Min Wu, Haifeng Gao, Devin Wu

¹Thermo Fisher Scientific, Eindhoven, The Netherlands

Poster Group 2

Direct quantitative investigation of the inner morphology and structure of soft materials is of critical importance to provide profound insights for properties evaluation. The scanning electron microscope (SEM) and focused ion beam (FIB), combined known as FIB-SEM or DualBeam, are conventionally recognized as a highly effective method to acquire 3D volume information. FIB-SEM together with integrated serial sectioning software has made the automated 3D data acquisition and analysis possible. However, slicing using Ga ion beam at room temperature has been found inducing severe damage to the beam sensitive soft materials, resulting in significant deterioration of the 3D data quality. Cutting edge cryogenic FIB-SEM technique provide a fully automated workflow which allows large volume, damage-free ion beam slicing and high spatial resolution SEM acquisition during serial sectioning under cryogenic conditions. With automated 3D reconstruction of the micrograph stacks, we can subsequently recover the comprehensive volume information of such beam sensitive materials. In addition, cryogenic multiple ion source PFIB has been confirmed to be capable of fabricating high quality large area TEM lamellae without damaging the beam sensitive bulk samples. Coupled with cryogenic in-situ nanomanipulator, the TEM samples can be easily lifted out under cryogenic conditions and subsequently transferred to TEM for further investigation. In this paper we present a series of large volume 3D imaging results and TEM sample preparation examples of extremely beam sensitive soft samples. The samples were processed on Thermo Scientific Helios 5 Hydra Plasma FIB platform with multiple ion species (Xenon, Argon, Oxygen and Nitrogen) combined with integrated state-of-the-art rotatable cryo stage. The slicing and imaging acquisition was achieved using the latest generation Automated Slice and View software and the subsequent data processing was conducted using Avizo 3D analysis and visualization software. The unique technical experiment set up and comprehensive application experience will be discussed in this presentation. In addition, inert gas transfer workflow of the beam sensitive materials from the plasma FIB to TEM will be discussed.

Keywords:

Cryogenic, beam sensitive, soft materials

766

Solvent-induced softening of polymethyl methacrylate surfaces

Dr James Bowen¹, Dr Simon Collinson

¹The Open University, Milton Keynes, UK

Poster Group 2

Background incl. aims

Exposing plastics to solvents is known to alter their surface and sub-surface properties, depending on the extent and duration of exposure. Amorphous plastics are prone to penetration and diffusion by low molecular mass solvents, leading to physical deformation including swelling, cracking, and dissolution. Unwanted or unexpected solid/liquid interactions can irretrievably compromise the visual characteristics of an object were it to be cleaned using an inappropriate method. This is of particular importance to the heritage and conservation sector, who use solvent-based cleaning systems to preserve the appearance of culturally-important artworks over many decades. There is increasing interest in the applicability of nanocharacterisation techniques to inform remedial conservation strategies for plastic artworks, supporting the preservation of the original intent of the artists and designers.

Methods

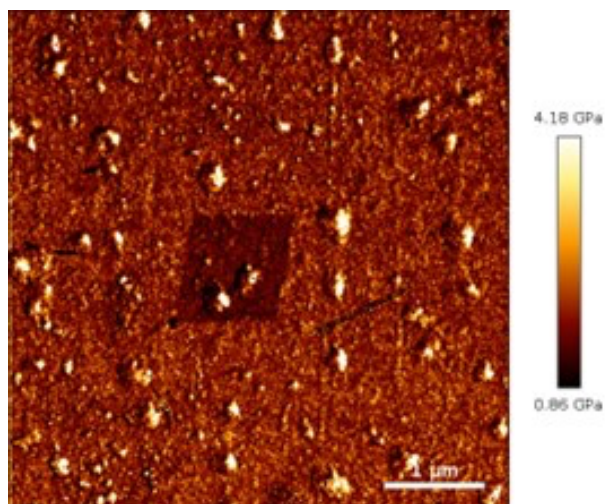
Polymethyl methacrylate (PMMA) is an important plastic in modern art and design collections, having been used since the mid-20th Century for creating artworks but also aircraft cockpit hoods, automotive and architectural lighting, and even windows on deep-sea submersibles. According to Hildebrand solubility theory, PMMA does not dissolve in aliphatic alcohols such as ethanol.

Results

We report that nanomechanical mapping of PMMA surfaces exposed to liquid ethanol experienced a decrease in elastic modulus according to an approximately exponential relationship. Further, interrogated regions of the surface were observed to have their mechanical properties altered because of the compressive load applied during the measurement process (Fig. 1).

Conclusion

These findings, which are of use to heritage and conservation scientists, also suggest opportunities for developing novel micro- and nanofabrication strategies, whereby a surface which has been temporarily and reversibly softened can be manipulated topographically, for example using nanolithography, nanoscratching, or nanoindentation.



Keywords:

ethanol, modulus, PMMA, polymer, solvent

Cellulose-based Nanocomposites for Sensor Applications: Characterization and Performance Evaluation

Asst. Prof. Domagoj Belić¹, Assoc. Prof. Mislav Mustapić¹, M.Sc. Dino Galić¹, B.Sc. Barbara Špigl¹, B.Sc. Sara Stivi¹, Assoc. Prof. Željko Skoko², Ph.D. Teodoro Klaser³, Assoc. Prof. Md Shahriar Al Hossain⁴

¹Department of Physics, J. J. Strossmayer University of Osijek, Osijek, Croatia, ²Department of Physics, Faculty of Science, University of Zagreb, Zagreb, Croatia, ³Ruđer Bošković Institute, Zagreb, Croatia, ⁴Faculty of Engineering, Architecture and Information Technology, The University of Queensland, Brisbane, Australia

Poster Group 2

Background including aims: Cellulose, an abundant and renewable natural polymer, offers extensive opportunities for diverse applications in materials science due to its favorable properties [1,2]. In this context, nanocomposite materials combining cellulose or its derivatives with nanoparticles such as Fe₃O₄, Au, Ag, and TiO₂, emerge as versatile platforms for sensor development. For instance, the characteristics of nanocellulose-water interactions can be exploited for the fabrication of flexible humidity sensors [3]. This study aims to create nanocomposite sensors specialized for detecting humidity and volatile organic compounds (VOCs) exploiting the synergistic effects of nanoparticles within the fibrillated nanocellulose or cellulose acetate matrix. Additionally, we investigate the potential of these nanocomposites for UV photodetection in flexible sensor systems.

Methods: We utilize different approaches for synthesizing fibrillated nanocellulose, cellulose acetate, nanoparticles of Fe₃O₄, Au, Ag, or TiO₂, as well as the related nanocomposites, aiming to integrate nanoparticles into flexible cellulose matrices [4]. Advanced electron microscopy techniques including conventional and low-dose Transmission Electron Microscopy (TEM), high- and low-vacuum Scanning Electron Microscopy (SEM), Focused Ion Beam (FIB) sectioning and Energy-Dispersive X-ray Spectroscopy (EDX) mapping are employed for precise characterization of nanocomposite morphology, structure and nanoparticle distribution. Humidity and VOC sensing experiments, along with UV photodetection tests, are conducted in the custom-built sensing system to evaluate sensor performance.

Results: TEM analysis reveals the precise morphology and dispersion of nanoparticles within the cellulose matrix at the nanoscale, highlighting the homogeneity crucial for sensor efficiency. SEM results, including cross-sectional profiling, provide detailed microstructural insights and, in combination with EDX, elucidate the spatial distribution of nanoparticles. Our nanocomposite-based sensors demonstrate notable sensitivity, selectivity, and response time towards varying humidity levels and diverse VOCs, as well as promising UV detection capabilities [5].

Conclusion: This study advances nanocomposite-based sensor technology by exploring the complex relationship between nanoparticle composition, nanoparticle distribution within cellulose matrix, and sensor performance. The findings underscore the potential of these multifunctional nanocomposites for diverse sensor applications, including humidity, VOC, and UV detection in flexible sensor platforms, thus paving the way for next-generation sensing technologies.

Keywords:

Nanocellulose, Metallic Nanoparticles, Nanocomposites, Sensors

Reference:

[1] Li, T.; Chen, C.; Brozena, A. H.; Zhu, J. Y.; Xu, L.; et al. Developing fibrillated cellulose as a sustainable technological material. *Nature* 2021

- [2] Thomas, B.; Raj, M. C.; B, A. K.; H, R. M.; Joy, J.; et al. Nanocellulose, a Versatile Green Platform: From Biosources to Materials and Their Applications. *Chemical Reviews* 2018.
- [3] Solhi, L.; Guccini, V.; Heise, K.; Solala, I.; Niinivaara, E.; et al. Understanding Nanocellulose–Water Interactions: Turning a Detriment into an Asset. *Chemical Reviews* 2023.
- [4] Mustapić, M.; Nedeljković, R.; Masud, M. K.; Alothman, A. A.; et al. Magnetic Nanocellulose: Influence of Structural Features on Conductivity and Magnetic Properties. *Cellulose* 2023
- [5] Belić, D.; Galić, D.; Špiĝl, B.; Stivi, S.; Mustapić, M.; et al. Integrating Metallic and Metal-oxide Nanoparticles into Cellulose-based Matrices for Flexible Sensors, submitted

1021

Morphological characterization of the electric field aligned block copolymers containing liquid crystal moiety

Monika Król¹, Isaac Álvarez Moisés², Janne Ruokolainen¹, Jean-François Gohy²

¹Aalto University, Espoo, Finland, ²Université catholique de Louvain, Louvain-la-Neuve, Belgium

Poster Group 2

Background incl. aims

Block copolymers (BCP) arose to be an interesting class of materials for the energy storage application. The conventional system consist of at least two covalently bound homopolymer blocks which are usually thermodynamically incompatible. It results in the phase separation at nanoscale, providing a wide array of self-assembled morphologies. Nanostructured periodically spaced discrete regions of different phases are characterized by respective properties similar to the pure homopolymers.

Solid polymer electrolytes (SPE) are composed of salt dissolved in a polymeric host. Here, BCPs are an attractive choice as a matrix due to the aforementioned qualities. Phase separation enables the possibility of merging intuitively contradictive functionalities in one material: solid state electrolyte with competitive to liquid alternative ionic conductivity, and mechanical stability. It is achieved by connecting the soft block which has ability to solvate the salt and favors ion transport, with rigid block, ensuring robustness. The length scale and type of the obtained microstructure can be swiftly tuned by careful molecular design of the polymer, including molecular weight, chain architecture, relative volume fractions, number and type of the constituent blocks. However, the phase separation itself is not the only requirement for BCPs sufficient performance as battery component. Due to the membrane thickness, the final structure is mostly isotropic and consists of multiple grains with different spatial orientation. This forces to consider not only intragrain ion transport, but also intergrain to fully understand the material performance as SPE. Liquid crystalline block copolymers (LC BCP) could be the pathway to manipulate the nanochannels orientation and ensure grain continuity. The addition of the mesogenic groups to the system allows to influence diamagnetic and dielectric constant properties of the materials, giving the promise of the highly ordered structures upon subjecting the material to external electric or magnetic fields. The main objectives of this study were to investigate the native hierarchical microstructure of LC BCP and to identify the self-assembled morphologies during solvent casting without and with the applied electric field. The analyzed material is composed of soft, ion conducting block and high glass transition temperature block with LC moiety. Both pristine and LiTFSI salt doped systems were structurally analyzed, as it was expected that addition of the ion to the matrix may change the system response to the external stimuli. As the next step, we examined alignment, grain size along with orientation and phase behavior of diblock copolymers while subjected to the applied (either alternating current (AC) or direct current (DC)) electric field during film casting. We also related both aligned and non-aligned electrolytes performance in terms of ionic conductivity to derive how the material morphology translates to its application as SPE.

Methods

Morphological characterization of the BCP was performed by means of SAXS (Small angle X-ray Scattering) and cryoTEM (cryogenic Transmission Electron Microscopy). SAXS provided statistical information of the BCP microstructure and alignment, whereas TEM provided more insight regarding the grain size and magnitude of the long-range order. Ionic conductivity was investigated by impedance spectroscopy.

Results

Phase separated BCP of conventional morphologies were obtained, where the hierarchical self assembly at two length scales was recognized (LAM-in-HEX for salt doped and LAM-in-LAM for

pristine). The addition of salt to the BCP caused phase transition from lamellar morphology to hexagonal, which can easily be explained by the swelling of the conductive phase due to solvating of the salt and hence actively increasing its volume fraction. Salt/BCP composites casted in presence of electric field resulted in increase of the ionic conductivity of the system by magnitude. Samples casted in AC field were characterized by perpendicular alignment of BCP in regards to the applied electric field and small grain size, whereas samples casted in DC field showed similar tendency in direction of reorienting the grains. However, the domain size was significantly increased.

Conclusion

The spatial grain orientation and size of BCP containing liquid crystal moiety was manipulated both via in DC and AC field, resulting in enhancement of the longer-range order and grain continuity. The increase of the ionic conductivity can be directly correlated to beneficial influence of electric field on the nano-channels alignment, which was proven by means of SAXS and TEM. This work highlights the importance of designing the nanostructured system which is susceptible to electric field directed self-assembly for BCP to find wide application in the energy storage field.

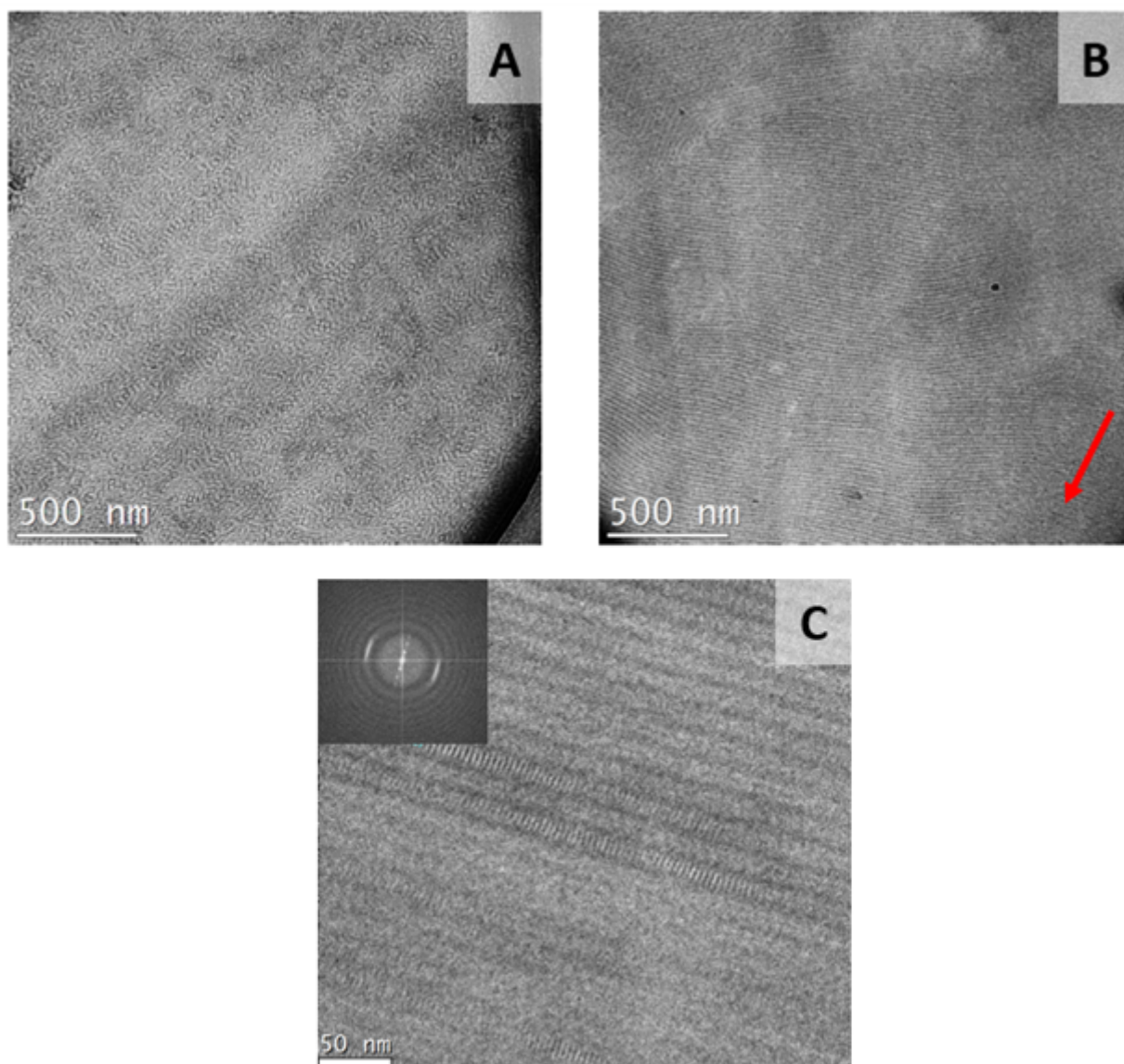


Figure 1. Bright-field micrographs depicting LiFTSI doped electrolyte consisting of conductive and LC containing blocks: A) Poorly ordered worm-like microstructure of BCP casted without EF alignment, B) Highly ordered HEX microstructure of BCP aligned via DC E_f . The red arrow indicates the direction of the applied electric field. C) Depiction of hierarchical microstructure of LC BCP, where lamellar-in-hexagonal structure can be observed

Keywords:

Solid polymer electrolytes, liquid crystals

Reference:

- [1] Gopinadhan, M. et al. (2017), Controlling orientational order in block copolymers using low-intensity magnetic fields, *Proceedings of the National Academy of Sciences*, 114, 201712631, 10.1073/pnas.1712631114.
- [2] Chao, Ch-Y. et al. (2004), Orientational Switching of Mesogens and Microdomains in Hydrogen-Bonded Side-Chain Liquid-Crystalline Block Copolymers Using AC Electric Fields, *Advanced Functional Materials*, 14, 364 – 370, 10.1002/adfm.200305159.
- [3] Pester, Ch. et al. (2017), Block Copolymers in Electric Fields, *Progress in Polymer Science*, 64, 182–214, 10.1016/j.progpolymsci.2016.04.005.

1047

Cryo-EM as a tool for observing alginate-based hydrogels

Katerina Mrazova^{1,2}, Anna Havlickova², Diana Cernayova², Kamila Hrubanova¹, Petr Sedlacek², Vladislav Krzyzaneck¹

¹Institute of Scientific Instruments of the CAS, v. v. i., Brno, Czech Republic, ²Faculty of Chemistry, Brno University of Technology, Brno, Czech Republic

Poster Group 2

Background

Hydrogel is an organic-based material, which finds its use in various fields ranging from well-known employment in medicine (wound treatment, scaffolds,...) to rising involvement in agriculture (superabsorbents, controlled release of fertilisers,...)[1]. While hydrogels containing chemical fertilisers provide valuable nutrients directly, the unused nutrients remain in the soil, where they accumulate, which negatively influences biodiversity, soil fertility, etc [2]. An alternative approach relies on the use of biological fertilisers (bioinoculants) in the form of plant growth-promoting bacteria (PGPRs). PGPRs positively stimulate the growth of plants using several mechanisms (phytohormone production, nitrogen fixation,...), while simultaneously reducing the growth of pathogenic microorganisms or chelating heavy metals [3]. One of the PGPRs is *Azotobacter vinelandii*, a microorganism interesting not only for its plant growth-promoting properties but also for its production of various polymers. Namely polyhydroxyalkanoates (PHAs), biopolymers praised for their properties similar to petrochemical plastics, or alginate, polysaccharide capable of forming a hydrogel. *A. vinelandii* releases alginate to form a capsule around the cells, which protects them from drying out and from other hostile environmental conditions. The production of alginate is a significant advantage of using *A. vinelandii* as bioinoculant since there is no need to add the hydrogel-forming polymers to the bacteria for encapsulation, the polymer already in the media is crosslinked and the resulting hydrogel is then processed into the final form of bioinoculant suitable for employment in agriculture [4]. This work aimed to study the morphology of hydrogel formed using different crosslinking agents (namely CaCl₂ and glucono-D-lactone), a step necessary to determine the most suitable crosslinker. Since alginate hydrogels are composed of polysaccharides and a substantial amount of water, chemical processing for EM could severely alter the hydrogel ultrastructure. Therefore, cryogenic fixation followed by freeze-fracture and cryo-SEM was proposed to be the most promising technique to study the polymeric net the most closely to the native state.

Methods

Cultures of *A. vinelandii* were cross-linked using various agents (2% CaCl₂, 1M GDL + 0,5M CaCO₃). The resulting hydrogels were cut using a scalpel to fit into 6mm carriers for high-pressure freezing and fixed using EM ICE (Leica Microsystems). No cryoprotectant was added. Frozen samples were transferred under liquid nitrogen into a cryo-vacuum preparation chamber (ACE600 Leica Microsystems), where they underwent freeze-fracturing followed by sublimation at -95°C for 7min. Samples containing hydrogel-encapsulated bacteria were then imaged in a scanning electron microscope (Magellan 400/L, FEI) equipped with a cryo-stage, at -120 °C using a 1–2 keV electron beam.

Results

Cryo-SEM imaging revealed cells of *A. vinelandii* containing polymeric granules, consisting of polyhydroxyalkanoate (PHA). As was previously proved, PHAs in the form of intracellular granules stay elastic even at temperatures of liquid nitrogen. They can be seen as needles sticking out of the freeze-fractured cells, as was visible also for *A. vinelandii*. Hydrogel encapsulating the cells showed different structures for both crosslinking agents. While hydrogel formed using CaCl₂ showed a net of

individually distinguishable fibres, the gel formed by GDL showed a dense mass surrounding cells. The changes in hydrogel ultrastructure seen in cryo-SEM support the difference in the macromorphological structure of the hydrogels visible immediately after cross-linking. Some polymer net was visible also for not crosslinked samples, possibly because of the trace concentration of Ca^{2+} ions in the cultivation media for the cells. However, the density of the net in the images as well as the overall amount of hydrogel was considerably lower. Similar results, supporting the hypothesis, were also obtained in the preliminary STEM experiments for freeze-substituted samples.

Conclusion

Cryo-SEM together with high-pressure freezing was proven to be a capable method for studying the structure of hydrogels. It was possible to determine the changes in the hydrogel structure based on the type of crosslinker used. Since the preliminary STEM data supported the cryo-SEM findings it is proposed to use the combination of these methods for the evaluation of other types of hydrogels.

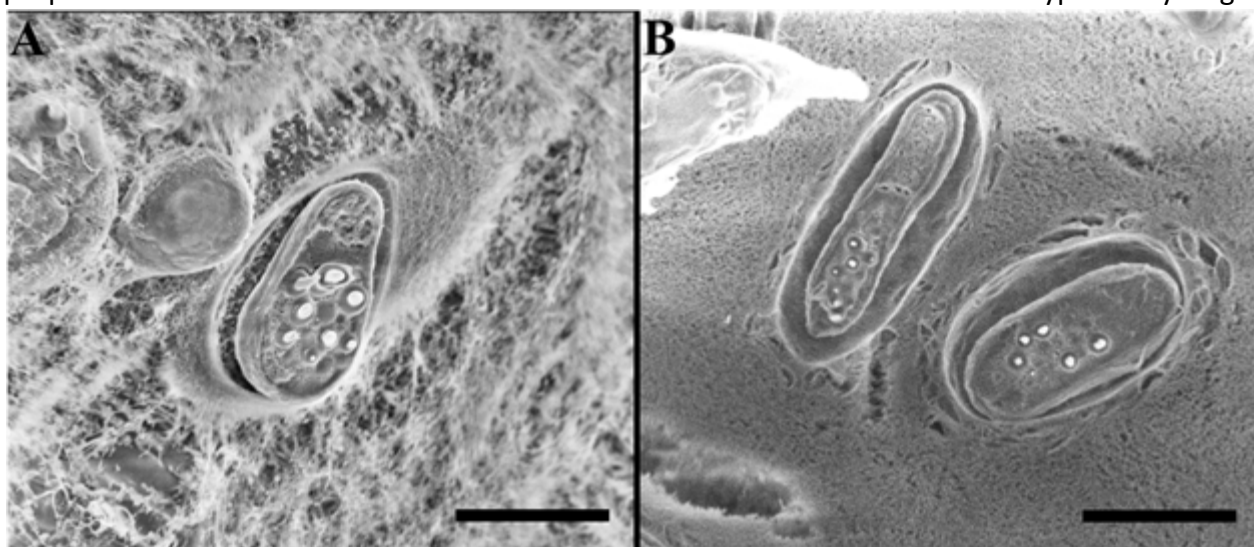


Fig.1: A. *vinelandii* cells encapsulated in the alginate-based hydrogel. Crosslinking agents used A) 2% CaCl_2 , B) 1M GDL + 0,5M CaCO_3 . PHB granules can be seen as needle sticking out of freeze fractured cells. Scalebar $3\mu\text{m}$

Keywords:

Hydrogel, alginate, bacteria, freeze-fracture, cryo-SEM

Reference:

- [1] Ahmed E. M. et al.: Journal of Advanced Research 6(2015), p. 105-121.
- [2] Bai Y.C. et al.: Microorganisms 8(2020), p. 694.
- [3] Santos M. S. et al.: AMB Express 9(2019), p. 205.
- [4] Noar J. D. et al.: Microbiology 164(2018), p. 421-436.

Acknowledgement: This work was supported by GACR (project GA23-06757S), and TACR (project TN02000020). Microscopic analysis was provided by CF ISI EM which is supported by the Czech-BioImaging large RI project (LM2023050 funded by MEYS CR).

1081

Analysis of the local chain orientation in conjugated polymer films

Mr Timothy Lambden¹, Dr Joonatan Laulainen¹, Dr Maximilian Moser², Dr Christina Kousseff², Professor Iain McCulloch^{2,3}, Dr Scott Keene^{4,5}, Professor Paul Midgley¹

¹Department of Materials Sciences and Metallurgy, University of Cambridge,, Cambridge, United Kingdom, ²Department of Chemistry, Chemistry Research Laboratory, University of Oxford, Oxford, United Kingdom, ³Department of Electrical and Computer Engineering, Engineering Quadrangle, 41 Olden Street, Princeton, USA, ⁴Electrical Engineering Division, Department of Engineering, University of Cambridge, Cambridge, UK, ⁵Cavendish Laboratory, University of Cambridge, , Cambridge, UK

Poster Group 2

Background incl. aims

Conjugated polymers have applications in organic, flexible electronics, with their mobility and conductivity largely dependent on parameters such as crystallinity, grain size, and chain orientation [1]. However, probing their structure at the nanoscale with electron microscopy remains challenging due to their radiation-sensitive nature. Development of fast direct electron detectors has helped open up the studies of these materials, with HRTEM and 4D-STEM data highlighting order and at the nanoscale not possible from x-ray approaches [2,3,4]. In this work we use low-dose scanning electron diffraction (SED), a variant of 4D-STEM, to investigate the nanoscale structure of conjugated polymers, with a workflow for determining chain orientation of conjugated polymers presented. We determine quantitatively chain orientation and grain size and compare to bulk experiments to observe how these quantities effect the underlying properties of the conjugated polymers.

Methods

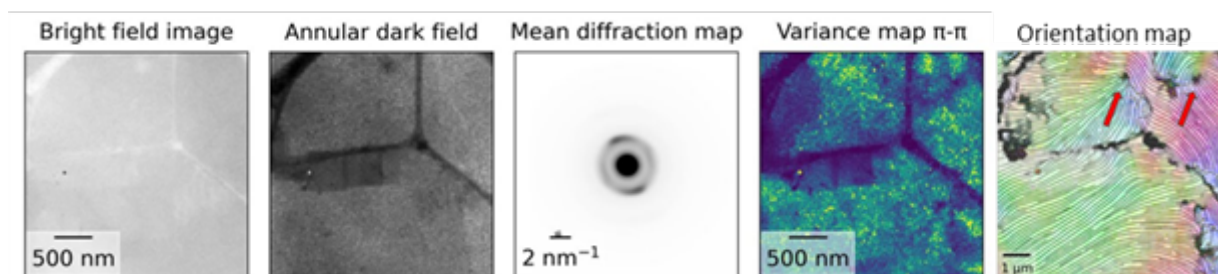
TEM samples of a thiophene-based conjugated polymer – with potential to be used as an organic mixed ionic-electronic conductors (OMIEC) [4] – were prepared via spin-coating and a lift-off approach onto Quantifoil, amorphous carbon grids. SED data, comprised of diffraction patterns (256 x 256 pixels), acquired over a raster scan of 256 x 256 pixels was acquired on a Thermo Fisher Spectra at 200 keV, with a low convergence angle of 1 mrad and with 5pA probe current. Each diffraction pattern was acquired using a Quantum Detectors Merlin camera and analysed using the pyXem software suite. Polymer chain orientation is visualised using ‘flowline maps’ based upon the orientation of Bragg spots due to π - π stacking in the conjugated polymer structure.

Results

The results from one of the polymers studied, p(gOT2-g6T2), is shown in Figure 1 to illustrate the analysis now possible of conjugated polymer thin films. The bright field (BF) image results from using a ‘virtual’ aperture placed around the direct beam in each of the patterns acquired and plotting the summed intensity as a function of probe position. The annular dark field image is plotted similarly but using a virtual annular aperture with radius range 0.25 Å⁻¹ – 0.3 Å⁻¹. The mean diffraction map is proportional to the summation of all the diffracted intensity across the field of view, with a bright spot present in the bottom left due to a hot pixel on the detector during acquisition. The ‘variance’ map plots the variation in scattered intensity in a narrow annulus centred on the strong Bragg ‘ring’ (corresponding to π - π stacking) – in essence this highlights areas of strong crystallinity / order. The final map illustrates the variation in chain orientation across the field of view through the use of a colour wheel (to plot the local Bragg vector for π - π stacking) and flow lines to illustrate more graphically the local polymer structure. In particular, here we highlight (see arrows) the appearance of disclinations (with $k = +1/2$ topology), commonly seen in polymer liquid crystals. By careful analysis of the ‘texture’ around the disclination core, quantitative measurements of the splay and bend characterisitcs may be determined.

Conclusions

The advent of 4D-STEM techniques, coupled with the progress in detector technology and the rise of computational power, provides an ideal platform for the study of conjugated polymers at lengthscales considerably smaller than is possible with other techniques such as x-ray diffraction. In the example we present here, chain orientation, grain size and the presence of disclinations have all been observed in the conjugated polymer p(gOT2-g6T2). The authors thank the EPSRC for funding under grant number EP/R008779/1.



Keywords:

Conjugated polymers, SED, 4D-STEM, low-dose

Reference:

- [1] Sirringhaus H. 25th anniversary article: organic field-effect transistors: the path beyond amorphous silicon. *Advanced materials*. 2014 Mar;26(9):1319-35.
- [2] Panova O, Ophus C, Takacs CJ, Bustillo KC, Balhorn L, Salleo A, Balsara N, Minor AM. Diffraction imaging of nanocrystalline structures in organic semiconductor molecular thin films. *Nature materials*. 2019 Aug;18(8):860-5.
- [3] Cendra C, Balhorn L, Zhang W, O'Hara K, Bruening K, Tassone CJ, Steinrück HG, Liang M, Toney MF, McCulloch I, Chabinyc ML. Unraveling the unconventional order of a high-mobility indacenodithiophene–benzothiadiazole copolymer. *ACS Macro Letters*. 2021 Oct 5;10(10):1306-14.
- [4] Keene ST, Laulainen JE, Pandya R, Moser M, Schnedermann C, Midgley PA, McCulloch I, Rao A, Malliaras GG. Hole-limited electrochemical doping in conjugated polymers. *Nature Materials*. 2023 Sep;22(9):1121-7.

1175

In-situ liquid-cell dynamic TEM observations of liquid crystal nanocomposite phase transitions

Ms Olga Kaczmarczyk¹, Katarzyna Matczyszyn¹, Andrzej Żak¹

¹Institute of Advanced Materials, Faculty of Chemistry, Wrocław University of Science and Technology, Wrocław, Poland

Poster Group 1

Background incl. aims

Liquid crystals (LCs) possess distinctive, anisotropic optical properties, and because of their fluidity combined with a partially ordered structure, they are easily influenced by external stimuli, making them extensively utilised in technology. The primary techniques used for their examination include polarised light microscopy (PLM), differential scanning calorimetry (DSC), small angle X-ray scattering (SAXS), and nonlinear optical imaging methods. Transmission electron microscopy (TEM) is known for its exceptional resolution and analytical capabilities. Although liquid crystals have been recognised for more than a century, only one study has reported TEM imaging of liquid crystals in their native state in the air [1]. This is partly due to the high vacuum environment of microscopes. To observe dynamic processes in a liquid environment, samples must be isolated from the vacuum, as imaging under high pressure leads to electron scattering and vacuum pump issues, hindering conventional TEM methods [2]. Another challenge, particularly for hydrated samples such as liquid crystals, is the impact of the electron beam, which requires precise control over the electron dose for reliable results.

Methods

In our study, we investigated the liquid crystal 4'-Octyl-4-biphenylcarbonitrile (8CB) and its nanocomposite that contains gold nanoparticles using polarizing microscopy and in-situ liquid-cell TEM.

Results

Our findings demonstrated the possibility of studying not only the arrangement of nanomaterials within the matrix but also the phase transitions kinetics of liquid crystal using the liquid-cell TEM approach. Polarising microscopy revealed changes in the optical properties of the nanocomposites upon the addition of Au nanomaterials, along with a uniform distribution of defects in the smectic A mesophase. We will discuss these results along with sample preparation for liquid-cell electron microscopy, the interaction between the electron beam and the sample, and dynamic observations of phase transitions.

Conclusion

Observations of LCs phase transitions and nanoparticle dynamics within the LCs matrix using TEM are possible with specified electron dose restrictions. Electron beam damage at low doses was negligible, and the phase transition was fully reversible. The dynamic behaviour of nanoparticle aggregates in LCs is linked to the electron dose value.

Keywords

Liquid-cell, TEM, in-situ, liquid crystals, nanocomposites

1231

Self-assembled nanoparticles in a thin film of water

Dr Crispin Hetherington¹, Dr Dmitry Baranov², Dr Katarzyna Makasewicz³

¹nCHREM, Lund University, Lund, Sweden, ²Chemical Physics and NanoLund, Lund University, Lund, Sweden, ³Institute for Chemical and Bioengineering, ETH Zürich, Zürich, Switzerland

Poster Group 1

Background including Aims

Metal nanoparticles that are functionalised may be used as markers in Cryo-EM studies on soft materials (Ahmad 2022). An observation has been made where these particles have self-assembled into remarkably regular 2-dimensional lattices in a thin water layer, and where the interparticle separation is large. The aim is to investigate this phenomenon, the role of the water thickness, and to link it to similar observations

Methods

Au nanoparticles functionalised with NH₂ groups were obtained from a commercial supplier and mixed with small unilamellar vesicles in a series of aqueous samples. TEM grids were prepared in the Leica GP1 grid plunger and transferred to the TEM in a Cryotransfer holder (Fischione Model 2550). Observations were made on a JEOL 2200FS TEM adapted for cryogenic studies and operated at 200 kV. While the main study was aimed at the interaction of the functionalised NPs with the vesicles, this presentation concerns the observation of the interaction between the functionalised NPs themselves.

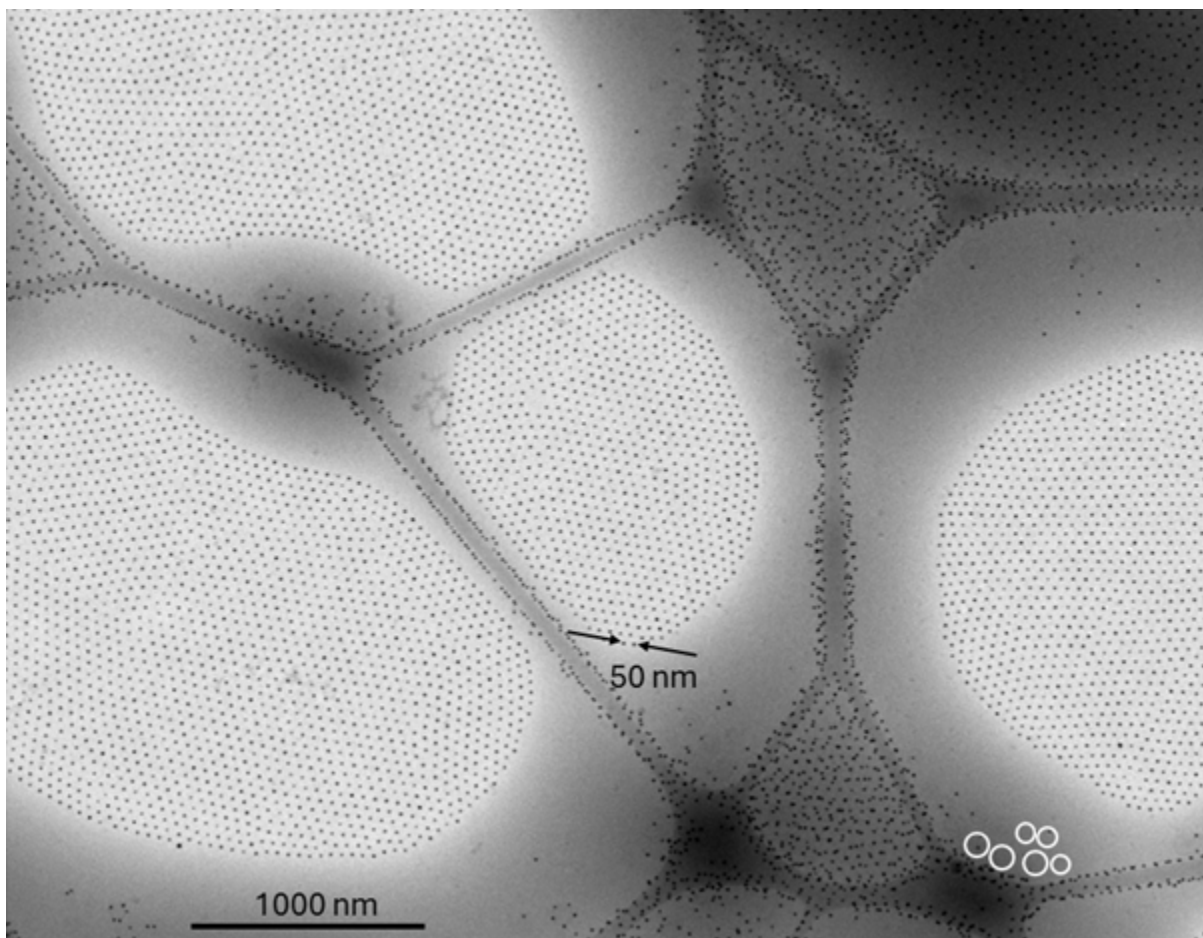
Results

Functionalised NPs were found to have self-assembled into a 2D hexagonal lattice. The interaction occurred only within thin layers of water. Note that the observations were made when the sample was frozen and the thin layer transformed to vitreous ice. The distance from one particle centre to another is in the 50 nm range, while the gold nanoparticle diameter is around 14 nm. Hence the gap between NP surfaces is around 36 nm, indicating a chain length of the functionalising ligand of around 18 nm.

Conclusions

Low density ordered arrays of particles forming spontaneously from various solutions are an interesting phenomenon. Previous work (Kanie 2012) found assemblies with 7 nm gaps between particles, which the authors commented was rather larger than typical gaps of 3 nm or even less. This observation of a 36 nm interparticle gap, which can still result in a particle array having a highly regular hexagonal packing, is intriguing. Further work will investigate the role of the thickness of the water/ice layer.

Figure 1 Micrograph showing self-assembled Au NPs in several patches of thin vitreous ice (200kV, TEM magnification 10kx). The distance between these NPs is around 50 nm. NPs can also be seen in thicker ice in random arrangements, and attached to the strands of lacey carbon film. Some small unilamellar vesicles appear (with low contrast in this image) in the thicker ice with sizes 70 - 100 nm; 6 are outlined in white.



Keywords:

Self-assembly Cryo-EM nanoparticles

Reference:

Ahmad, F.; Salem-Bekhit, M.M.; Khan, F.; Alshehri, S.; Khan, A.; Ghoneim, M.M.; Wu, H.-F.; Taha, E.I.; Ibagory, I. Unique Properties of Surface-Functionalized Nanoparticles for Bio-Application: Functionalization Mechanisms and Importance in Application. *Nanomaterials* 12, 1333 (2022)

Kiyoshi Kanie, Masaki Matsubara, Xiangbing Zeng, Feng Liu, Goran Ungar, Hiroshi Nakamura and Atsushi Muramatsu *J. Am. Chem. Soc.* 134, 2, 808–811 (2012)

1322

Electron Energy-Loss Spectroscopy of Liquids

Sofie Tidemand-Lichtenberg¹, Shima Kadkhodazadeh¹, Kristian Speranza Mølhave¹

¹Technical University of Denmark, Kgs. Lyngby, Denmark

Poster Group 1

Background incl. aims

Liquid phase transmission electron microscopy (LPTeM) makes it possible to study reactions and dynamics in liquids at atomic resolution, with application in biology, battery studies, catalysis etc. This makes it a powerful tool for understanding the underlying mechanisms of liquid phase processes and interactions with other liquids or solids.

Electron energy loss spectroscopy (EELS) enables elemental analysis of materials through energy measurements in the transmission electron microscope (TEM). From EELS measurements it is possible to extract not only the elemental composition, but also obtain chemical bond knowledge of the electronic structures from the energy-loss near-edge structure (ELNES).

Combining LPTeM with EELS makes it possible to examine the elemental composition of liquids as well as their electronic structure and thereby chemical bonding structure through the ELNES.

Additionally, it will enable the analysis of the beam induced changes in sample chemistry in the liquids and can be a valuable tool to understand radiolysis of liquids.

The aim of this study is firstly to measure, analyze and understand the molecular structure of a range of different liquids through their EELS spectra with associated ELNES structures, and assess if there are prominent radiolytic effects of the beam on liquid.

Methods

Nanochannel LPTeM chips of silicon nitride, supplied by InsightChips, were used to encapsulate the water. The nanochannels allow flow and thereby exchange of liquids while inserted in the TEM and makes it possible to have thin layers of liquids, thereby enhancing the resolution of the EELS spectrum compared to other silicon nitride based LPTeM systems. Graphene based LPTeM methods do not allow flow and hence cannot be used to establish a baseline measurement where there is a need for continuous fresh supply of the liquid to avoid radiolytic effects.

To obtain a sufficiently high resolution to resolve the ELNES structure of the water a Spectra Ultra S/TEM with a monochromator was used in for the measurements in both scanning transmission electron microscopy (STEM) and TEM mode. When the beam was focused on one of the channels it was possible to generate bubbles through radiolysis, which was then analyzed using the EELS system on the microscope. This allows us a better understanding of the liquid – electron beam interaction. The bubbles are temporary and dissolve in minutes if not continuously irradiated.

Results

From the oxygen edge on the core-loss spectrum it is possible to extract information about the structure of the water. Additionally, it is possible to determine the molecular composition of the radiolytic gases generated from the interaction between the liquid and the electron beam. Finally, it has been possible to evaluate the structure of other liquids such as ethanol and hexane.

Conclusion

From the experimental measurements of liquids, we present an approach for determination of the structures of different liquids. Additionally, the aim was to obtain knowledge of the radiolytic processes that occur in liquids when exposed to a high dose electron beam.

Keywords:

LPTeM, EELS, liquid analysis.